AN ANALYSIS OF THE PRESSURE DROP AND VOID
FOR A TWO-PHASE SLUG FLOW IN INCLINED PIPES

by

Loren Swan Bonderson

B.S.M.E., University of Nebraska
(1967)

SUBMITTED IN PARTIAL FULFILLMENT

OF THE REQUIREMENTS FOR THE

DEGREE OF MASTER OF

SCIENCE

at the

MASSACHUSETTS INSTITUTE OF TECHNOLOGY

January, 1969

Signature of Author..
Department of Mechanical Engineering, January 20, 1969

Certified by..
Thesis Supervisor

Accepted by..
Chairman, Departmental Committee on Graduate Students

ABSTRACT

AN ANALYSIS OF THE PRESSURE DROP AND VOID
FOR A TWO-PHASE SLUG FLOW IN INCLINED PIPES

by

Loren Swan Bonderson

Submitted to the Department of Mechanical Engineering on January 20, 1969, in Partial Fulfillment of the Requirements for the Degree of Master of Science

A model of two-phase slug flow in inclined pipes is proposed. A typical bubble and slug combination is described by: A bubble nose of changing cross section determined by a constant pressure Bernoulli equation, a middle section of constant cross section determined by force equilibrium, a horizontal tail section, and a liquid slug of length proportional to the pipe size. The model predicts the total pressure gradient due to the sum of gravity and wall shear stresses. An investigation of the relationship between pressure gradient and pipe size results in an optimum pipe size at which the pressure gradient is minimized. Preliminary comparisons between model predictions of pressure gradient and published experimental results show a -25% systematic error and a ± 15% deviation.

Thesis Supervisor: Peter Griffith

Title: Professor of Mechanical Engineering

ACKNOWLEDGEMENTS

The author sincerely thanks his thesis supervisor Professor Peter Griffith who has been an ever available source of inspiration and assistance, and Miss Pamela Beecher who typed the manuscript.

The author's college education has been subsidized by individuals, organizations, and both state and federal government. To all of these my everlasting gratitude.

TABLE OF CONTENTS

LIST OF FIGURES

NOMENCLATURE

A		Pipe cross section area, in ft^2.
A_f		Liquid cross section area, in ft^2.
A_g		Gas cross section area, in ft^2.
D		Pipe diameter, in ft.
F		Dimensionless fraction defined in Eq. (42).
f		Fanning friction factor, dimensionless.
f_g		Fanning friction factor for gas phase, dimensionless.
Fr	=	V^2/gD, dimensionless Froude number.
Fr'		Modified Froude number defined Eq. (49).
G		Mass velocity, in lbm/sec ft^2.
g		Acceleration of gravity, in ft/sec^2.
G_f		Liquid mass velocity, in lbm/sec ft^2.
G_g		Gas mass velocity, in lbm/sec ft^2.
g_o		Gravitational constant, in ft lbm/sec^2 lb_f.
K_1		Dimensionless model parameter defined in Eq. (32).
K_2		Dimensionless model parameter defined in Eq. (9).
K_3		Dimensionless model parameter defined in Eq. (10).
L	=	$L_b + L_s$, in ft.
L_b		Bubble length, in ft.
L_s		Slug length, in ft.
P		Pressure, in lb_f/ft^2.
P_f		Wetted pipe perimeter, in ft.
Q_f		Liquid volume flow rate, in ft^3/sec.

Q_{fe}	Effective liquid volume flow rate, in ft^3/sec.
Q_g	Gas volume flow rate, in ft^3/sec.
Q_{ge}	Effective gas volume flow rate, in ft^3/sec.
R	Pipe radius, in ft.
Re	Dimensionless Reynolds number defined in Eq. (21).
R_{gg}	Dimensionless ratio of gas shear force and liquid gravity force.
V	Mixture velocity, in ft/sec.
V_1	Velocity at point or section number 1, in ft/sec.
V_2	Velocity at point or section number 2, in ft/sec.
V_b	Bubble rise velocity with respect to liquid ahead of bubble, in ft/sec.
V_f	True liquid velocity, in ft/sec.
V_f'	True liquid velocity relative to bubble velocity, in ft/sec.
V_g	True gas velocity, in ft/sec.
V_g'	True gas velocity relative to the bubble velocity, in ft/sec.
V_{gf}	True gas velocity relative to the liquid velocity, in ft/sec.
Vol	Bubble volume, in ft^3.
X	Quality, dimensionless.
x	Coordinate, in ft.
x'	Coordinate, in ft.
z	Coordinate, in ft.
z_b	Maximum z-coordinate of bubble, in ft.

Greek Symbols

α	Void fraction, dimensionless.
β	Angle of inclination from horizontal.
η_f	Liquid kinematic viscosity, in ft^2/sec.
θ	Cross section angle, in radians.
ν_1	Specific volume at section number 1, in ft^3/lbm.
ν_2	Specific volume at section number 2, in ft^3/lbm.
ρ_a	Average density, in lbm/ft^3.
ρ_f	Liquid density, in lbm/ft^3.
ρ_{fe}	Effective liquid density, in lbm/ft^3.
ρ_g	Gas density, in lbm/ft^3.
τ	Shear stress between pipe and liquid, in lb_f/ft^2.
τ_{gf}	Shear stress between gas and liquid, in lb_f/ft^2.

Delta Quantities

Δh	Vertical distance, in ft.
ΔL	Increment of L, in ft.
ΔL_b	Increment of L_b, in ft.
ΔP	Total pressure gradient, in lb_f/ft^3.
ΔP_f	Friction pressure gradient, in lb_f/ft^3
ΔP_g	Gravity pressure gradient, in lb_f/ft^3
ΔP_m	Momentum pressure gradient, in lb_f/ft^3.
$\Delta\rho$	$= \rho_f - \rho_g$, in lbm/ft^3.
Δt	Period of time, in sec.
ΔVol	Increment of Vol, in ft^3.

Δx	Increment of x, in ft.
$\Delta x'$	Increment of x', in ft.
Δz	Increment of z, in ft.

1. INTRODUCTION

Current techniques for designing gas and oil pipelines often fail to give good pressure drop predictions for flow in inclined pipes. The correlation due to Martinelli[(1)*] makes no allowance for the effect of hills on the friction pressure drop. The Martinelli correlation computes the friction pressure drop as a multiplier times a single-phase pressure drop. Thus, this method always predicts a wall friction which is opposite to the direction of net flow. However, for two-phase flow in inclined pipes the local wall friction, and possibly the net wall friction, can be either direction. This is possible because there can exist a net liquid flow upward but still be regions of flow in which the liquid is running down the pipe wall. See Reference (2).

Various modifications of the Martinelli method have been made but the author knows of no correlation which will predict this effect of wall friction.

It is suggested that for two-phase flow in inclined pipes there is an optimum pipe size. The total pressure drop increases as the pipe size is either increased or decreased from this optimum size. Unfortunately almost all experimental work has been for a constant pipe size with the weight flow rates of the two phases being varied. This is just the opposite of the situation faced by a pipeline

---

*Superscript numbers are referred to in the Bibliography.

designer. Here the flow rates are specified and the designer chooses a pipe size to minimize pumping and construction costs.

Thus, the existence of an optimal pipe size has not been clearly demonstrated due to a lack of proper experimental work. However, for the case of vertical two-phase flow the data of References (2) and (3) can be cross plotted for one condition of gas and liquid flow rates. The result is shown in Figure 1. Guzhov[4] also recognizes the existence of an optimum pipe size. A plot of total pressure drop versus average velocity of the mixture shows a minimum pressure drop. This is actually the same phenomenon as previously mentioned since if the gas and liquid flow rates are held constant, a change in average velocity corresponds roughly to a change in pipe size. Note that this is only roughly the same effect since the specific flow geometries are at least not obviously identical. Guzhov also states that another optimum case exists if the point of view of specific energy is considered; that is to minimize the energy expenditure per unit of pumped mixture. However, for the practical design situation the gas and liquid flow rates should be considered as fixed and thus the only degree of freedom in the optimization is the total pressure drop.

The validity of the assumption of slug flow at the minimum pressure drop is based on the visual observations of Grovier[2] [3] and the fact that the void fraction predicted by slug flow considerations agrees very well with the experimental results of Reference (4).

The object of this thesis is very limited compared to most of the early and current work being done in two-phase flow. While many investigators have sought one general correlation between two-phase pressure drop and the system variables for all flow regimes, this work concerns itself solely with slug flow in an upward flowing inclined pipe. Bubbly flow will be considered as the limiting case of slug flow for very small gas flow rates or as a developing pattern which will ultimately develop into slug flow.

Thus, some knowledge of when slug flow becomes wave or cresting flow and eventually an annular or mist flow is desired. Unfortunately, the author knows of no comprehensive mapping of flow regimes for inclined flow. For the case of vertical flow Griffith(5) indicates that slug or bubble flow exists for all $Fr \leq 12.$ for $Q_g/(Q_g + Q_f) \cong 1.0$ and for all $Fr \leq 80.$ for $Q_g/(Q_g + Q_f) \cong 0.0$. For the case of inclined flow Brigham(6) observed slug flow whenever $Fr \leq 170.$ at an incline of 5.5° from the horizontal and whenever $Fr \leq 400.$ at an incline of 12.4° from the horizontal. These results were reported in terms of G_f and G_g. The average pressure of the tests varied considerably and thus an exact conversion of the results to Fr is not possible.

The question that this work will attempt to answer is very simple: Given the flow rates as being fixed and the geometry of the system, what is the size of pipe to minimize the pressure drop?

A model of two-phase slug flow in inclined pipes will be proposed and its characteristics throughly investigated. The model will be based on visual observations and on experimental results of the most fundamental nature. After the development of the model a criterion will be derived indicating for what combination of Fr and inclination of flow the model is capable of representing the true flow condition.

2. THEORY

2.1 Assumptions

The following assumptions are basic to the model to be proposed and are presented here in total for completeness:

1. Surface tension forces in the force balance are assumed to be negligible. However, the bubble rise velocity expression will be based on a correlation, due to Zukoski[9], which includes the effect of surface tension. This assumption allows the interface between gas and liquid to be taken as horizontal at any pipe section. See Figure 2. This assumption is good for air and water in the slug flow regime and improves for the case of natural gas and oil which have a smaller surface tension.
2. At any pipe section each phase is assumed to be characterized by a single velocity. This allows the use of one-dimensional equations and greatly simplifies any continuity calculation. This assumption can be made with good accuracy for turbulent flow, which one has in slug flow.
3. Any pressure drop due to gas wall shear stress and gas weight is neglected. Thus, the gas in any one bubble is assumed to be at a constant pressure and the gas-liquid interface for any one bubble is at a constant pressure. This assumption is good whenever the density of the gas is small compared to the density of the liquid and the

velocity of the gas is of the same order of magnitude as the velocity of the liquid. This assumption also includes neglecting any interfacial shear force. However, the increase of this interfacial shear is one of the causes of the transition from slug flow to annular flow as the flow rates are increased.

4. The tail of the bubble is assumed to be perfectly horizontal. Observations[(8) (9)] substantiate this approximately and it is expected that an increase in pipe size would improve this approximation.

5. The basic model assumes that there is no entrainment of the gas phase in the liquid phase. However, the flow quantities will later be modified to allow for this effect. This, in effect, allows a combination of both a slug and a bubbly flow model.

6. The density of both phases is assumed to be constant for purposes of continuity calculations.

7. The gas phase will be assumed to obey the ideal gas law when calculating a momentum pressure drop. This is a good approximation for small pressure gradients and even then, the momentum pressure drop will be shown to be negligible for flow conditions of interest.

8. A change of phase is assumed not to occur. Thus, evaporation, condensation, heating, and reactions are not allowed.

9. The gas and liquid mass flow rates and the pipe diameter and inclination are assumed to be constant.

10. For purposes of implementing the model or a computer the Fanning friction factor for smooth pipes will be used. The hydraulic diameter concept will be assumed to effectively account for the varying flow geometries. This is generally considered to give good results for turbulent flow but it is fundamentally wrong for laminar flow. However, the hydraulic diameter will be used to give approximate results for any small region in which the flow may be laminar.

2.2 Model Visualization

The proposed kinematic model of slug flow in inclined pipes is an extension of the model described by Griffith[5] and Stanley[7] for vertical slug flow. Photographs of slug flow in inclined pipes by Runge and Wallis[8] and Zukoski[9] show a situation similiar to the model visualization of Figure 2. The gas-liquid interface perpendicular to the plane of the illustration is horizontal as previously assumed.

Portion 1. of the bubble surface is a region of changing cross section at the nose of the bubble. By considering continuity the liquid velocity may be related to the fraction of the cross section occupied by liquid, but the velocity of the liquid may also be determined by writing a constant pressure Bernoulli equation for a streamline of liquid falling from the top of the bubble nose to any point on the gas-liquid interface. By combining these two relationships the shape of the bubble nose will be determined.

Portion 2. of the bubble surface is a mid-section of constant cross section. The shape of this cross section will be determined by requiring equilibrium to exist between gravity forces and wall shear forces acting on an element of liquid. The cross section shape is constant when this equilibrium exists because the liquid element is no longer experiencing a change of velocity.

Portion 3. is the bubble tail and is assumed to be a horizontal surface.

Other equations must be developed before specific equations for these curves can be derived.

2.3 Cross Section Geometry

With the previous assumptions a typical cross section in which both gas and liquid are flowing is shown in Figure 3.

The total area of the pipe is:

$$A = \pi R^2 \quad . \tag{1}$$

The angle Θ is a function of z, the distance from the top of the pipe to the gas-liquid interface, and is given by:

$$\Theta = \mathrm{ARC\ COS}\left(\frac{R - z}{R}\right) \quad ,$$

$$0 \leq \Theta \leq \pi \quad . \tag{2}$$

The area of the pipe occupied by the gas, A_g, and the area occupied by the liquid, A_f, are:

$$A_g = R^2(\Theta - \text{SIN}\Theta\text{COS}\Theta) \quad , \tag{3}$$

$$A_f = R^2(\pi - \Theta + \text{SIN}\Theta\text{COS}\Theta) \quad . \tag{4}$$

The perimeter of the pipe wetted by the liquid is:

$$P_f = 2R(\pi - \Theta) \quad . \tag{5}$$

2.4 Phase Velocities

With the preceding assumptions the continuity equation becomes:

$$(Q_f + Q_g)_1 = (Q_f + Q_g)_2 \quad . \tag{6}$$

This simply states that the total volume flow rate remains constant from one cross section to the next cross section.

At the entrance to the pipe the gas flow rate is constant at Q_g and the liquid flow rate is constant at Q_f. At a sufficient distance from the entrance the flow pattern characteristic of slug flow will become established and there will be no more coalescing of bubbles. Thus, if a cross section is considered between bubbles, the liquid must have a velocity V given by:

$$V = \frac{Q_g + Q_f}{A} \quad . \tag{7}$$

The velocity of the gas in the bubble is:

$$V_g = V + V_b \quad , \tag{8}$$

where V_b is defined to be the velocity of the bubble with respect to the velocity of the liquid between the bubbles.

Zuber[10] considers the general problem of phase velocities and volumetric concentrations of two-phase flow in vertical pipes. For the special case of slug flow the expression:

$$V_b = K_2 V + 0.35 \left(\frac{g \, \Delta\rho \, D}{\rho_f}\right)^{1/2} \quad , \tag{9}$$

is offered in agreement with previous investigators. Note carefully that V_b is a relative velocity in this thesis while in some publications V_b is defined as the total velocity of the bubble. This results in K_2 being smaller than some of the published constants by a factor of unity. A value of $K_2 = 0.20$ is offered by Zuber as a best approximation but it is shown to vary considerably and no indication of the effect of pipe inclination is given. For the purpose of this model the previous expression will be modified to account for the effect of pipe inclination:

$$V_b = K_2 V + 0.35 K_3 \left(\frac{g \, \Delta\rho \, D}{\rho_f}\right)^{1/2} \quad . \tag{10}$$

The two terms in this expression may be thought of as representing two distinct and separate phenomenon. The second term is the rise velocity of a bubble in a tube emptying experiment, since when the bottom of a tube filled with liquid is uncovered it empties so that $(Q_f + Q_g) = 0$. The model parameter K_3 then simply allows for a different tube emptying bubble rise velocity than the velocity in a vertical tube. The parameter is primarily a function of pipe inclination but is also dependent on other system variables. The value of K_3 may be found from Reference (9).

The first term in Eq. (10) is then any additional relative velocity the bubble may have when the mixture velocity V is non-zero. An oversimplified but still useful interpretation of the model parameter K_2 is that it is the fraction by which the velocity of the liquid directly ahead of the bubble nose is greater than the mixture velocity. One cause of this effect is that the liquid velocity is not perfectly uniform, thereby allowing the liquid velocity at a particular point to vary from the mixture velocity V. As stated previously, a value $K_2 = .20$ will be used in this model, but only because an adequate experimental determination has not been made.

The velocity of the liquid, V_f, at any cross section may be found using Eq. (6) and referring to Figure 4. Eq. (6) becomes:

$$VA = V_f A_f + V_g A_g \quad . \tag{11}$$

Substituting Eq. (8) and realizing that $A = A_g + A_f$, Eq. (11) may be solved for V_f:

$$V_f = V - V_b \frac{A_g}{A_f} \quad . \tag{12}$$

It is also of interest to consider the phase velocities with respect to a coordinate system moving with the bubble, that is with a velocity V_g. These relative velocities are:

$$V_{g'} = 0 \quad . \tag{13}$$

$$V_{f'} = -V_b \frac{A}{A_f} \quad . \tag{14}$$

2.5 Void Fraction

Consider a bubble and slug combination as shown in Figure (2). For the ideal case, all bubble and slug combinations are identical and all bubbles have the same velocity. The time required for such a bubble and slug combination to pass a fixed point on the pipe wall is:

$$\Delta t = \frac{L}{V_g} \quad . \tag{15}$$

In every Δt period of time one bubble of volume, Vol, passes. Thus, the volume flow rate of gas becomes:

$$Q_g = \frac{Vol}{\Delta t} \quad . \tag{16}$$

The void fraction, α, is defined to be the fraction of the total pipe volume occupied by the gas phase at any instant of time.

Thus, considering this typical bubble and slug combination:

$$\alpha = \frac{Vol}{L\ A} \quad . \tag{17}$$

Combining Eqs. (7), (8), (15) and (16) one obtains:

$$\frac{Vol}{L} = \frac{Q_g\ A}{Q_f + Q_g + V_b A} \quad . \tag{18}$$

Notice that the left hand side of this equation is a function of the bubble geometry while the right hand side is a constant determined by the system variables.

If Eqs. (17) and (18) are combined the void fraction becomes:

$$\alpha = \frac{Q_g}{Q_f + Q_g + V_b A} \quad . \tag{19}$$

2.6 Equilibrium Considerations

By Eq. (12) the velocity of the fluid depends on the ratio $\frac{A_g}{A_f}$. As A_f becomes very small, V_f will become a very large negative number, indicating liquid flow down the pipe. Since the liquid is flowing past a bubble at constant pressure, the net pressure force acting on the two ends of a thin cross section of liquid may be taken as zero. Thus, the only forces acting on the element of liquid are as shown in Figure 5. Since V_f is sensed positive up the pipe, τ, the shear stress acting on the liquid, will be sensed positive down the pipe so as to oppose liquid flow and τ will always have the same sign as V_f. The liquid cannot accelerate down the pipe when the forces acting along the pipe come into equilibrium, that is when:

$$A_f \, \Delta L \, \rho_f \, \frac{g}{g_o} \, \text{Sin}\,\beta = -\tau \, P_f \, \Delta L \quad ,$$

which simplifies to:

$$\tau \frac{P_f}{A_f} = -\rho_f \frac{g}{g_o} \, \text{Sin}\,\beta \qquad (18)$$

The shear stress may be expressed in terms of the Fanning friction factor f, as:

$$\tau = f \, \rho_f \, \frac{V_f^2}{2 \, g_o} \quad , \qquad (19)$$

where f is a function of a Reynolds number based on a hydraulic diameter:

$$f = f(\text{Re}) \quad , \qquad (20)$$

$$\text{Re} = \frac{4 \, V_f \, A_f}{P_f \, \eta_f} \quad , \qquad (21)$$

and f has the same sign as V_f to keep the correct sign convention on τ. Eq. (18) then becomes:

$$\frac{f \, V_f^2 \, P_f}{A_f} = -2g \, \text{Sin}\,\beta \quad . \qquad (22)$$

If the function $f(Re)$ is specified and the values of K_2 and K_3 are determined then Eqs. (1), (2), (3), (4), (5), (7), (10), (12), (20), (21), and (22) can in principle be solved for the unique value of z, $0 \leq z \leq D$, at which equilibrium is achieved. This value of z will be called z_b.

2.7 Interface Equations

Consider the flow of liquid past a rising bubble as viewed from a reference frame moving with the bubble. Following the method of Taylor[11], the Bernoulli equation for steady flow along a streamline lying at the constant pressure, gas-liquid interface may be written:

$$\frac{V_2^2}{2g} = \frac{V_1^2}{2g} + \Delta h \quad , \tag{23}$$

where the subscripts refer to positions shown in Figure 5, and Δh is the vertical distance between the two positions. From Figure 5, Δh is seen to be:

$$\Delta h = x \operatorname{Sin} \beta + z \operatorname{Cos} \beta \quad . \tag{24}$$

At the top of the bubble nose, the relative velocity is zero, and the relative velocity V_2 is:

$$V_2 = V_f{}' = -V_b \frac{A}{A_f} \tag{25}$$

Thus, Eq. (23) can be written as:

$$\frac{\left(V_b \frac{A}{A_f}\right)^2}{2g} = x \text{ Sin } \beta + z \text{ Cos } \beta \quad . \tag{26}$$

But from Eq. (1), (2) and (4) for $z = 0$, $A_f = A$ and the above equation becomes:

$$\frac{V_b^2}{2g \text{ Sin } \beta} = x \quad , \tag{27}$$

giving a finite positive value of x when $z = 0$. This is clearly not desired and arises because the problem was assumed to be one-dimensional.

This problem can be alleviated by at least two simple approaches, both giving the same resulting equation. The velocity V_1 can be set equal to the average relative velocity of the liquid in a cross section at the bubble nose, that is $V_1 = -V_b$. Eq. (23) then becomes:

$$\frac{\left(V_b \frac{A}{A_f}\right)^2 - V_b^2}{2g} = x \text{ Sin } \beta + z \text{ Cos } \beta \quad . \tag{28}$$

The second solution is to retain Eq. (26) as correct, but to neglect the undesired distance given by Eq. (27). This amounts to moving the x origin to the location given by Eq. (27). Thus, in Eq. (26) the distance x is replaced by:

$$x + \frac{V_b^2}{2g \, \mathrm{Sin}\, \beta} ,$$

giving:

$$\frac{\left(V_b \dfrac{A}{A_f}\right)^2}{2g} = \left(x + \frac{V_b^2}{2g \, \mathrm{Sin}\, \beta}\right) \mathrm{Sin}\, \beta + z \, \mathrm{Cos}\, \beta ,$$

which is seen to be the same as Eq. (28).

Eq. (28) may then be solved for x as a function of z:

$$x = \frac{\left(V_b \dfrac{A}{A_f}\right)^2 - V_b^2}{2g \, \mathrm{Sin}\, \beta} - z \, \mathrm{Cot}\, \beta , \tag{29}$$

which will be taken as the equation of the bubble nose.

The x' coordinate system has its origin at the tail of the bubble, see Figure 2. In this coordinate system, which also moves with the bubble, the equation of the horizontal gas-liquid interface of the bubble tail is:

$$x' = z \, \mathrm{Cot}\, \beta . \tag{30}$$

Both Eqs. (29) and (30) are valid only for $z < z_b$ as found in Section 2.6. When z reaches a value z_b the bubble nose curve, Eq. (29), and the bubble tail curve, Eq. (30), are connected by a bubble mid-section of constant cross section. Thus, the cross section, see Figure 3, of this connecting portion has a gas-liquid interface that is a distance:

$$z = z_b \tag{31}$$

below the top of the pipe. Thus, Eqs. (29), (30) and (31) completely describe the gas-liquid interface.

The length of the liquid slug, L_s, will be taken as:

$$L_s = K_1 R \quad , \tag{32}$$

where K_1 is a model parameter which must be determined by experimentation. For the case of vertical flow Griffith[5] found K_1 to vary considerably, but a value of $K_1 = 20.$ will be used as the best approximation until a more accurate determination is made.

If a Δz is given, Eqs. (30) and (31) may be used to find a ΔL_b where:

$$\Delta L_b = \Delta x + \Delta x' \tag{33}$$

An increment of bubble volume, ΔVol, is given by:

$$\Delta Vol = \Delta L_b A_g \quad , \tag{34}$$

where of course A_g is a function of z. Thus, when K_1, K_2, K_3 and z_b are determined, Eqs. (1), (2), (3), (4), (7), (10), (18), (29), (30), (31), (32), (33) and (34) constitute a complete set of equations that can be solved by numerical methods to find VOL and L_s. The numerical integration must proceed simultaneously along the bubble nose and tail, always keeping z the same value at both sections so that the two sections can in effect be joined together when Eq. (18) is satisfied. See the appendix for one solution.

2.8 Pressure Gradients

Consider a control volume as shown in Figure 6, which contains one bubble and slug combination and is fixed in space. The pressure indicated in Figure 6 is the average pressure acting on the cross section and ΔP is a pressure gradient, sensed so as to be positive for a decrease of pressure in the positive flow direction.

The average density, ρ_a, of the material contained in the control volume is:

$$\rho_a = \alpha \rho_g + (1-\alpha) \rho_f \quad . \tag{35}$$

Since the time rate of change of momentum in the control volume is zero, the momentum equation for forces along the length of the pipe is:

$$\Delta P \; AL - \Sigma \tau P_f \Delta L - \rho_a \frac{g}{g_o} AL \text{ Sin } \beta = \frac{A}{g_o} (\rho_2 V_2^2 - \rho_1 V_1^2) \quad . \tag{36}$$

Solving for ΔP:

$$\Delta P = \frac{\Sigma \tau P_f \Delta L}{AL} + \rho_a \frac{g}{g_o} \text{ Sin } \beta + \frac{\rho_2 V_2^2 - \rho_1 V_1^2}{L g_o} \quad . \tag{37}$$

This may also be written:

$$\Delta P = \Delta P_f + \Delta P_g + \Delta P_m \quad . \tag{38}$$

The term:

$$\Delta P_f = \frac{\Sigma \ \tau \ P_f \ \Delta L}{AL} , \qquad (39)$$

is the pressure gradient due to friction. The summation is to be taken along a length of pipe equal to L. This term can be evaluated by numerical methods using the results of Sections 2.6 and 2.7, and Eqs. (1), (2), (3), (4), (5), (7), (10), (12), (19), (20), (21), (29), (30), (31), (32), and (33). This may be accomplished simultaneously with the determination indicated in Section 2.7. See the appendix for one possible solution.

The term:

$$\Delta P_g = \rho_a \frac{g}{g_o} \ \text{Sin} \ \beta \qquad (40)$$

is the pressure gradient due to gravity. This term may easily be evaluated once K_2 and K_3 have been determined by using Eqs. (1), (7), (10), (19) and (35).

The term:

$$P_m = \frac{\rho_2 \ V_2^2 - \rho_1 \ V_1^2}{L \ g_o} , \qquad (41)$$

is the pressure gradient due to momentum. This term is neglected because it is very small for slug flow. The notation used is intended to be descriptive but not explicit. Refer to the appendix for an evaluation of this term assuming a homogeneous flow model. This method yields an answer of at least the correct order of magnitude.

2.9 Gas Entrainment

All of the preceding theory has been for a separated flow model in which each phase has a distinct velocity. However, there may be a significant amount of the gas phase entrained in the liquid phase and thus would have the same velocity as the liquid. The effect of this would be an increase in the effective liquid volume flow rate but a decrease in effective liquid density and effective gas volume flow rate.

Define F to be the fraction of the effective liquid volume flow rate which is actually gas flowing with the liquid. That is:

$$F = \frac{Q_{fe} - Q_f}{Q_{fe}} \quad , \tag{42}$$

where Q_{fe} is the effective liquid volume flow rate and Q_f is, as before, the true liquid volume flow rate. Solving for Q_{fe}:

$$Q_{fe} = \frac{Q_f}{1 - F} \quad . \tag{43}$$

By a conservation of mass and total mixture volume flow rate argument the equations for Q_{ge} and ρ_{fe} follow:

$$Q_{ge} = Q_g - \frac{F\, Q_f}{1 - F} \quad , \tag{44}$$

$$\rho_{fe} = F \rho_g + (1 - F) \rho_f \quad . \tag{45}$$

Thus, this effect is easily accounted for by replacing the system variables Q_f, Q_g and ρ_f by Q_{fe}, Q_{ge} and ρ_{fe} respectively.

3. THE VALIDITY RANGE OF THE MODEL

3.1 Interfacial Shear

One of the initial assumptions was that any interfacial shear force would be neglected, even though this force is one of the causes of the transition from slug flow to annular flow. This assumption was very important for the derivation of Eq. (22), repeated here:

$$\frac{f\ V_f^2\ P_f}{A_f} = -2g\ \mathrm{Sin}\ \beta \quad , \tag{22}$$

which was solved to find z_b.

To determine a criterion of when this assumption can be made, the ratio of gas shear force to gravity force will be evaluated at the value of z_b found from Eq. (22) using the method of Section 2.6. Thus, when this ratio, R_{gg}, becomes significant, Eq. (22) no longer represents a true equilibrium balance for an element of liquid.

The velocity of the gas with respect to the actual liquid velocity at the interface is:

$$V_{gf} = V_g - V_f = -V_f' = V_b \frac{A}{A_f} \quad . \tag{46}$$

The shear stress of the gas on the liquid may be expressed in terms of a Fanning friction factor as:

$$\tau_{gf} = f_g\ \rho_g\ \frac{V_{gf}^2}{2g_o} \quad . \tag{47}$$

Referring to Figure 3 and 5, the area on which this shear stress acts is $2R\ \Delta L \sin \Theta$. Thus, the ratio R_{gg} may be written:

$$R_{gg} = f_g \frac{\rho_g V_b^2 A^2 R \sin \Theta}{\rho_f A_f^3 g \sin \beta} \quad . \qquad (48)$$

To simplify this analysis, both f and f_g will be assumed to be constant and equal to .005, the value which is correct for $Re = 6 \times 10^4$. Eq. (22) was solved for z_b and Eq. (48) was then evaluated at z_b for the range of system variables:

R	=	.03435 ft.
Q_g	=	.026 - .150 ft^3/sec.
Q_f	=	.0024 - .0068 ft^3/sec.
ρ_g	=	.075 lbm/ft^3.
ρ_f	=	62.24 lbm/ft^3.
β	=	1^o - 90^o.

The resulting values of R_{gg} correlate very well with a modified Froude number:

$$Fr' = \frac{\rho_g}{\rho_f} \frac{V^2}{g D \sin \beta} \quad . \qquad (49)$$

The relationship was found to be:

$$Fr' = 34.4 R_{gg} \quad . \qquad (50)$$

Thus, to keep $R_{gg} \leq .10$ would require that:

$$\frac{\rho_g}{\rho_f} \frac{V^2}{g \ D \ \text{Sin} \ \beta} \leq 3.44 \quad .$$

The range of system variables was chosen to correspond to the data of Reference 12.

3.2 Void Fraction

Guzhov[4] gives an experimental relationship between the void fraction, α, and the two variables, Fr and $\frac{\rho_g}{\rho_g + \rho_f}$, for a pipe inclination of $\beta = 9^o$. The correlation is intended to account for the effect of pipe size so unfortunately the pipe sizes used in the experiment are not stated.

The dependence of α on the same variables as predicted by Eqs. (1), (7), (10), and (19) was determined. A value of $R = .03435$ ft. was used and K_3 was determined from Reference 9. The result was a similiar relationship but the value of K_2 was still variable, and thus could be used to bring the two results into exact agreement.

The best value of K_2 varied in the following way:

Fr	K_2
.1	.09
.4	.12
.8	.08
2	.08

Fr	K_2
4	.10
16	.19
50	.20
80	.20
100	.20

for the entire range of $\frac{Q_g}{Q_g + Q_f}$, except for Fr $\geq$ 50 and $\frac{Q_g}{Q_g + Q_f} \cong 1$ when the following values were needed:

Fr	K_2
50	.15
80	.12
100	.10

The fact that the experimental results could be perfectly matched by a simple choice of K_2 indicates that the analysis used is reliable. Note that within experimental error the value of K_2 appears to be either .08 or .20 except for a small range at $\frac{Q_g}{Q_g + Q_f} \cong 1$.

4. RESULTS

A computer realization of the proposed model is given in the appendix. The program was written to run on an IBM 1130. The notation used in the program is in most cases similar to the notation used in this thesis. A listing of equivalent symbols and abbreviations preceeds the program to make it self-explanatory.

The characteristics of this model are illustrated in Figures 7 through 14. The same set of system variables and model parameters was used for each illustration. These were:

SYSTEM VARIABLES

$\beta = 10^{\circ}$

$Q_f = .02 \ ft^3/sec.$

$Q_g = .10 \ ft^3/sec.$

$\rho_f = 62.24 \ lbm/ft^3$

$\rho_g = .075 \ lbm/ft^3$

$\eta_f = 1 \times 10^{-5} \ ft^2/sec.$

MODEL PARAMETERS

$K_1 = 20.$

$K_2 = .20$

$K_3 = 1.00$

$F = 0.0$

The pressure gradients ΔP_g, ΔP_f, ΔP_m and the total pressure gradient, ΔP, for the basic set of variables are shown in Figure 7. The model clearly predicts an optimum pipe size for which the total pressure gradient is a minimum. ΔP_m is negligible compared to ΔP_f as expected. The pressure gradient due to friction becomes a small negative number for all $R > .11$ ft. but does approach zero as R becomes still larger. Thus, the total pressure gradient is caused only by gravity for large R and approaches the value for a pipe filled with static liquid:

$$\Delta P_g = \rho_f \frac{g}{g_o} \operatorname{Sin} \beta = 10.8 \ lb_f/ft^3 .$$

For a value of $R_{gg} \leqq .10$ the results of Section 3.1 indicate that the model is valid for $R > .034$ ft.

The effect of varying the model parameters one at a time is illustrated in Figure 8, 9, 10 and 11. Each of the parameters is varied over as extreme a range as could reasonably be anticipated. While all of the parameters have an effect on the total pressure gradient and thus need to be accurately determined, the parameters K_3 and F have the most pronounced effect on the location of the minimum while K_2, K_3 and F have the greatest effect on the magnitude of the pressure gradient. The parameters K_1, K_2 and F have the interesting characteristic of reversing their effect on the pressure gradient as the pipe size changes.

The relationships between the total pressure gradient and the system variables Q_f, Q_g and β, as predicted by the model, are shown in Figures 12, 13 and 14. All of the variables have a pronounced effect on the total pressure gradient and the location of the minimum. It should be carefully noted that a value of $Q_g = 0.$ in Figure 13 indicates that there is only liquid in the pipe and thus, a pipe of infinite size is needed to minimize the pressure gradient because ΔP_g remains a constant for a pipe running full of liquid. However, in Figure 12 a value of $Q_f = 0.$ does not indicate the absence of liquid, only that the net movement of the liquid in the pipe is zero.

The experimental data of Reference 12 was filtered using the criterion established in Section 3.1 with a value of $R_{gg} \leq .09$ which requires that $Fr' \leq 3.1$. This resulted in all data taken for $\beta = 0^o$ and the higher flow rates taken at small angles being unacceptable for this model. The model was then used to predict the pressure gradient for the remaining data. The range of system variables was as noted in Section 3.1. The model parameters used were:

$$K_1 = 20.$$
$$K_2 = .20$$
$$K_3 = 1.00 - 1.34$$
$$F = 0.0$$

The specific value of K_3 for each angle of inclination was determined from Reference 9. The comparison of the measured pressure gradient versus the predicted pressure gradient is shown in Figure 15. For this choice of model parameters the model has a systematic error of -25% and a deviation of about $\pm$ 15% assuming that the experimental data is correct. It should be noted that these results were obtained assuming smooth pipe Fanning friction factors. No attempt was made to alter the friction factor or the model parameters to obtain a better agreement.

5. DISCUSSION

An examination of Figure 12 indicates that for any fixed pipe size the pressure gradient always increases as Q_f is increased. However, this is not the case for the gas flow rate Q_g. In Figure 13 at a fixed pipe size of $R = .05$ it is easily seen that the pressure gradient first decreases and then increases again as the gas volume flow rate is increased from zero. Thus, a value of Q_g which minimizes the pressure gradient for this pipe size is seen to exist. The trend of Figure 13 suggests that a similar phenomenon would be observed at every pipe size if the value of Q_g were allowed to increase sufficiently. Both of these effects have been substantiated by many experimentors for the case of vertical flow.

The model then exhibits all of the characteristics observed in two-phase slug flow. If the model can be shown to predict the correct magnitude of the pressure gradient it will be a considerable improvement over correlation schemes since this model has the advantage of being based on model parameters of physical significance whereas correlation schemes are not closely related to physical quantities. A first comparison between predicted pressure gradient and experimentally measured pressure gradients[(12)] is presented in Figure 15. The measured pressure gradients were reported to have an error not greater than 10%. The few flow conditions for which more than one pressure gradient was reported tend to substantiate such a deviation but no estimate can be made of any systematic error. The pressure gradients were measured using pressure transducers and then the fluctuating pressure traces were averaged by manual techniques. This method is much better than using damped manometers which can be shown to be non-linear devices for a constantly fluctuating pressure. An even better technique would have been to average the output of the transducer by electronic methods.

All of the measured pressure gradients were for flow conditions that correspond to a pipe size smaller than the predicted optimum and thus had a large friction pressure gradient compared to the gravity pressure gradient. Thus, all of the data points were for flow conditions close to the transition from slug to annular flow and did not constitute a really good test of this model. It is hoped that more experimental work will be done in the slug flow regime in the future.

The four model parameters, K_1, K_2, K_3 and F need to be experimentally determined. The model parameter K_1 as shown in Figure 8 has an almost negligible effect on the pressure gradient, and thus does not need to be accurately determined. The relative insensitivity of the model to this parameter justifies the original assumption that the bubble tail is perfectly horizontal, because the most important effect of the tail being slightly different from horizontal is an effective change in the length of the liquid slug.

The parameters K_2, K_3 and F all have significant effects on the pressure gradient. The parameter K_3 is currently well correlated[(9)] and F is expected to be close to zero for slug flow and only become significant when there is a considerable amount of mixing and churning in the flow pattern. Thus, the parameter K_2 is of greatest interest if the model is expected to give accurate results.

The parameter K_2 can be experimentally determined by measuring either the velocity of a bubble, V_g, or the void fraction, α, if F is assumed to be zero and K_3 is assumed to be known. The velocity of a bubble could be electronically determined by inserting two small circuit elements into the top portion of a pipe a known distance apart. Each element would be designed to act as a short circuit when surrounded by liquid and an open circuit when surrounded by the gas of a bubble. The signals from such sensors could be interpreted to yield bubble velocity, bubble length, and slug length. This experiment would appear to be much simplier and accurate than an experiment to measure the void fraction.

If the equation for V_g and α are examined closely as they would appear for a non-zero value of F it is seen that if the tube emptying bubble velocity, the total gas velocity, and the void fraction are measured independently then in theory a unique set of model parameters K_2, K_3 and F is determined. However, the accuracy needed would probably be impossible to obtain to yield a meaningful value of F.

that actually result in slug flow except for angles very close to horizontal. The flow visualization becomes obviously wrong as the inclination approaches vertical. The existence and extent of any limitation of the model for large angles of inclination has not yet been determined.

After observing the characteristics of this model it is concluded that the effect of varying the pipe size can not easily, if at all, be predicted by varying the flow rates at a constant pipe size. Thus, it is urged that the effect of pipe size be investigated using one experimental apparatus so that all pressure and void measurements are made with the same equipment and thus provide self-consistant data.

The model is dependent on the four parameters K_1, K_2, K_3 and F, and can only be accurate if these parameters are accurately known. Currently, only K_3 is well correlated with the flow but fortunately K_3 is the most critical for locating the minimum pressure gradient.

BIBLIOGRAPHY

1. Lockhart, R.W., and R.C. Martinelli, "Proposed Correlation of Data for Isothermal Two-Phase, Two-Component Flow in Pipes," Chem. Eng. Progr., 45, p. 39 (1949).

2. Grovier, G.W., B.A. Radford, and J.S.C. Dunn, "The Upward Vertical Flow of Air-Water Mixtures I. Effect of Air and Water Rates on Flow Pattern, Holdup and Pressure Drop," Can. J. Chem. Engr., 35, p. 58 (1957).

3. Grovier, G.W., and W.L. Short, "The Upward Vertical Flow of Air-Water Mixtures II. Effect of Tubing Diameter on Flow Pattern, Holdup and Pressure Drop," Can. J. Chem. Engr., 36, p. 195 (1958).

4. Guzhov, A.I., V.A. Mamayev, and G.E. Odishariya, "A Study of Transportation in Gas-Liquid Systems," 10th International Gas Conference, Hamburg, 1967.

5. Griffith, P., and G.B. Wallis, "Two-Phase Slug Flow," Trans. ASME, J. Heat Transfer, 83, p.307, (1961).

6. Brigham, W.E., "Two-Phase Flow of Oil and Air Through Inclined Pipe," M.S. Thesis, University of Oklahoma (1956).

7. Stanley, D.W., "Wall Shear Stress in Two-Phase Slug Flow," M.S. Thesis, Massachusetts Institute of Technology (1962).

8. Runge, D.E., and G.B. Wallis, "The Rise Velocity of Cylindrical Bubbles in Inclined Tubes," Technical Report No. NYO-3114-8, Dartmouth College, Hanover, N.H. (1965).

9. Zukoski, E.E., "Influence of Viscosity, Surface Tension, and Inclination Angle on Motion of Long Bubbles in Closed Tubes,' J. Fluid Mech., 25, P. 821 (1966).

10. Zuber, N., and J.A. Findlay, "Average Volumetric Concentration in Two-Phase Flow Systems," Trans. ASME, J. Heat Transfer, 87, p. 453 (1965).

11. Davis, R.M., and G.I. Taylor, "The Mechanics of Large Bubbles Rising Through Extended Liquids and Through Liquids in Tubes," Proc Royal Soc, V200, Series A, p. 375 (1950).

12. Sevigny, R., "An Investigation of Isothermal, Co-Current, Two-Fluid, Two-Phase Flow in an Inclined Tube," Ph.D. Thesis, University of Rochester, Rochester, N.Y. (1962).

13. O'Donnell, J.P., "11th Annual Study of Pipeline Installation and Equipment Costs," Oil and Gas J, 66, (1968).

APPENDIX A

The pressure gradient due to momentum was expressed as:

$$\Delta P_m = \frac{\rho_2 V_2^2 - \rho_1 V_1^2}{L g_o} .$$

It is not at all clear what the expressions for these densities and velocities should be for a separated flow model. However, to determine an answer of at least the correct order of magnitude, a homogeneous flow model may be used to calculate ΔP_m.

Thus:

$$\Delta P_m = \frac{G^2 (\nu_2 - \nu_1)}{L g_o}$$

or if ν_2 is evaluated at a distance $L = 1$ ft. from the point were ν_1 is evaluated, this becomes:

$$\Delta P_m = \frac{G^2 (\nu_2 - \nu_1)}{g_o}$$

where

$$G = \frac{\rho_g Q_g + \rho_f Q_f}{A} .$$

For homogeneous flow the quality, X, is:

$$X = \frac{\rho_g Q_g}{\rho_g Q_g + \rho_f Q_f} .$$

Thus, the specific volume of the homogeneous mixture before any pressure drop is:

$$\nu_1 = \frac{X}{\rho_g} + \frac{(1 - X)}{\rho_f}$$

The density of the gas at section 2, 1 ft. along the pipe from section 1 is:

$$\rho_{g2} = \rho_g \frac{P - \Delta P(1\ ft)}{P}$$

for a gas obeying the ideal gas law. The pressure P is the average absolute pressure at which the flow is occurring. Thus, assuming that the liquid does not have a density change, the specific volume of the homogeneous mixture at section 2 is:

$$\nu_2 = \frac{X}{\rho_{g2}} + \frac{(1 - X)}{\rho_f} \quad .$$

These equations may then be used to calculate ΔP_m when a pressure gradient ΔP exists. The first value of ΔP to be used would not include the ΔP_m term, but then must be changed to include ΔP_m and the solution repeated until no change occurs in ΔP.

APPENDIX B

Functions defined in the computer program are:

FAG(Z), calculates A_g for any value of z.

FPF(Z), calculates P_f for any value of z.

TAU (AG, PF), calculates τ for any value of A_g and P_f.

The Fanning friction factor used to calculate τ is for smooth pipes and is approximated by the three relations:

$$f = \frac{16}{Re}, \qquad Re \leq 2 \times 10^3.$$

$$f = \frac{.0791}{(Re)^{.25}}, \quad 2 \times 10^3 < Re \leq 2 \times 10^4.$$

$$f = \frac{.046}{(Re)^{.20}}, \quad 2 \times 10^4 < Re.$$

The variables used in the program correspond to previously defined terms as indicated or are defined below:

Program Name	Definition
A	A
AF	A_f
AG	A_g
ALPHA	α
AVP	Average pressure at which the flow is occurring, in psia.
BETA	β

BETAP	BETA for printout.
DELF	Increment of F.
DELR	Increment of R.
DELXN	Δx
DELXT	$\Delta x'$
DELZ	Δz
DP	ΔP
DPB	Friction pressure gradient from a length L_b.
DPF	ΔP_f
DPGR	ΔP_g
DPM	ΔP_m
DPS	Friction pressure gradient from a length L_s.
DVOL	Increment of Vol.
EPSIA	EPSI 1 } Entered differently.
EPSIB	EPSI 2 } Entered differently.
EPSIC	EPSI 3 } Entered differently.
EPSI 1	Program parameter to determine accuracy of equilibrium location.
EPSI 2	Program parameter to determine size of Δz for integration along bubble.
EPSI 3	Program parameter to determine the allowable size of Δx and $\Delta x'$ in the closing of a solution.
F	F
FG	Force of gravity along the pipe for a typical length L.

FS	Friction force acting in a length L_s.
FST	The first value given to F.
G	G
I, II, J	Do loop indexes or counters.
K 1	K_1
K 2	K_2
K 3	K_3
L	L
LB	L_b
LS	L_s
NU	η_f at first, then becomes an effective η_f because of an effective density change.
NUS	Saved value of NU.
PF	P_f
QF	Q_f at first, then becomes Q_{fe}.
QFS	Saved value of QF.
QG	Q_g at first, then becomes Q_{ge}.
QGS	Saved value of QG.
QUAL	X
R	R
RE	Re
ROAV	ρ_a
ROF	ρ_f at first, then becomes ρ_{fe}.
ROFS	Saved value of ROF.
ROG	ρ_g

ROG 2	ρ_g at section 2, 1 ft. up pipe from section 1, where pressure has dropped (ΔP) (1 ft)
RR	R for printout.
RST	The first value given to R.
SK 1 SK 2 SK 3	K 1 K 2 } Entered differently K 3
SPV 1	ν_1
SPV 2	ν_2
SSTOP	STOP, Entered differently.
STOP	Indicates number of times R is incremented.
STOP 1	Indicates number of times F is incremented.
SUMFB	A sum which finally equals the friction force in a length L_b.
TAU	τ
THETA	θ
V	V
VB	V_b
VF	V_f
VOL	Vol
XN	x
XN 1	Previous value of XN.
XP	Length of the mid-section of bubble with a $z = z_b$.
XT	x'

XT 1	Previous value of XT.
YY 1, Y 1, Y 3	Names for groups of physical variables, used for convience.
Z	z
ZS	z_b

The program follows, with one page of output on which Figure 7 is based.

```
PAGE    1    BONDERSON

// JOB T                                                    BONDERSON

LOG DRIVE   CART SPEC   CART AVAIL  PHY DRIVE
  0000        0001        0001        0000

// FOR
*LIST SOURCE PROGRAM
C      FUNCTION FAG CALCULATES THE UPPER AREA OF THE PIPE CROSS SECTION.
C      (OCCUPIED BY GAS).
C      Z IS THE DISTANCE OF THE FLUID SURFACE BELOW THE TOP OF THE PIPE.
       FUNCTION FAG(Z)
       COMMON R,VB,A,V,NU,ROF
       THETA=ATAN(SQRT(2.*R*Z-Z*Z)/(R-Z))
       IF(R-Z)100,101,101
100    THETA=THETA+3.1415927
101    FAG=R*R*(THETA-SIN(THETA)*COS(THETA))
       RETURN
       END

CORE REQUIREMENTS FOR FAG
 COMMON      12  VARIABLES      12  PROGRAM      86

 END OF COMPILATION

// DUP

*STORE       WS  UA  FAG
D 06 ENTRY POINT NAME ALREADY IN LET/FLET


// FOR
*LIST SOURCE PROGRAM
C      FUNCTION FPF CALCULATES THE WETTED PERIMETER OF THE PIPE.
       FUNCTION FPF(Z)
       COMMON R,VB,A,V,NU,ROF
       THETA=ATAN(SQRT(2.*R*Z-Z*Z)/(R-Z))
       IF(R-Z)102,103,103
102    THETA=THETA+3.1415927
103    FPF=2.*R*(3.1415927-THETA)
       RETURN
       END

CORE REQUIREMENTS FOR FPF
 COMMON      12  VARIABLES      12  PROGRAM      78

 END OF COMPILATION

// DUP

*STORE       WS  UA  FPF
D 06 ENTRY POINT NAME ALREADY IN LET/FLET


// FOR
*LIST SOURCE PROGRAM
C      FUNCTION TAU CALCULATES THE WALL SHEAR STRESS FOR THE FLUID.
       FUNCTION TAU(AG,PF)
       REAL NU
```

```
PAGE   2    BONDERSON

      COMMON R,VB,A,V,NU,ROF
      AF=A-AG
      VF=V-VB*AG/AF
      RE=4.*ABS(VF)*AF/(PF*NU)
      IF(RE-2.0E3)104,104,105
105   IF(RE-2.0E4)106,106,107
104   TAU=(16.*ROF*(VF**2))/(RE*64.4)
      GOTO 108
106   TAU=(.0791*ROF*(VF**2))/((RE**.25)*64.4)
      GOTO 108
107   TAU=(.046*ROF*(VF**2))/((RE**.20)*64.4)
108   IF(VF)109,110,110
109   TAU=-TAU
110   RETURN
      END

CORE REQUIREMENTS FOR TAU
 COMMON      12  VARIABLES      12  PROGRAM    168

 END OF COMPILATION

// DUP

*STORE       WS   UA   TAU
D 06 ENTRY POINT NAME ALREADY IN LET/FLET


// FOR
*IOCS(CARD, 1132 PRINTER)
*NAME SLUG
* LIST SOURCE PROGRAM
C      THE DATA CARDS ARE AS FOLLOWS
C      1.  THE FIRST CARD IS BLANK IF K1,K2,K3 ARE TO BE SPECIFIED ON
C        THE INDIVIDUAL DATA CARDS.   IF K1,K2,K3 ARE TO BE SPECIFIED FOR
C        A GROUP OF DATA CARDS, THEY ARE ENTERED AS SK1,SK2,SK3 ON THE
C        FIRST DATA CARD IN 3E10.4 FORMAT.
C      2.  THE SECOND CARD IS BLANK IF EPSI1,EPSI2,EPSI3 ARE TO BE
C        SPECIFIED ON THE INDIVIDUAL DATA CARDS.  IF EPSI1,EPSI2,EPSI3
C        ARE TO BE SPECIFIED FOR A GROUP OF DATA CARDS, THEY ARE ENTERED
C        AS EPSIA,EPSIB,EPSIC ON THE SECOND DATA CARD IN 3E10.4 FORMAT.
C      3.  ON THE THIRD CARD ARE  SSTOP AND AVP IN 2E10.4 FORMAT.  SSTOP=
C        0. IF STOP IS TO BE SPECIFIED ON THE INDIVIDUAL DATA CARDS.
C        IF STOP IS TO BE SPECIFIED FOR A GROUP OF DATA CARDS, IT IS
C        ENTERED HERE AS SSTOP.
C      4.  ON THE FOURTH CARD ARE  FST,DELF,STOP1 IN 3E10.4 FORMAT.
C        FST=0. AND STOP1=1. UNLESS GAS ENTRAINMENT IS TO BE CONSIDERED.
C      5.  THE PARAMETERS OF A SINGLE FLOW CASE ARE ENTERED ON TWO DATA
C        CARDS.  ON THE FIRST CARD ARE  BETA,QF,QG,ROF,ROG,NU,DELR,RST IN
C        8E10.4 FORMAT.  ON THE SECOND CARD ARE  K1,K2,K3,EPSI1,EPSI2,
C        EPSI3,STOP IN 8E10.4 FORMAT.   NOTE THAT THIS SECOND CARD MAY
C        BE BLANK IF ALL THESE PARAMETERS ARE BEING SPECIFIED FOR THE
C        WHOLE GROUP OF DATA CARDS.
C      6.  THE LAST TWO DATA CARDS MUST BE BLANK TO END THE PROGRAM.
       REAL NU,L,LS,LB,K1,K2,K3,NUS
       COMMON R,VB,A,V,NU,ROF
       READ(2,198) SK1,SK2,SK3
       READ(2,198) EPSIA,EPSIB,EPSIC
       READ(2,198) SSTOP,AVP
       READ(2,198) FST,DELF,STOP1
 198   FORMAT(3E10.4)
```

```
199   READ(2,200) BETA,QF,QG,ROF,ROG,NU,DELR,RST,K1,K2,K3,EPSI1,EPSI2,
     1EPSI3,STOP
200   FORMAT(8E10.4)
C     THE MODEL EQUATIONS ARE NOT DEFINED FOR BETA=0. AND THUS BETA=0.
C     IS USED AS AN ENDING ROUTINE.
      IF(BETA-.00001) 406,406,409
409   IF(SK1-.00001) 411,411,410
410   K1=SK1
      K2=SK2
      K3=SK3
411   IF(EPSIA-.00001) 413,413,412
412   EPSI1=EPSIA
      EPSI2=EPSIB
      EPSI3=EPSIC
413   IF(SSTOP-.00001) 407,407,414
414   STOP=SSTOP
407   QFS=QF
      QGS=QG
      ROFS=ROF
      NUS=NU
      F=FST
      BETA=BETA*3.1415927/180.
      DO 417 J=1,20
      AJ=J
      IF(AJ-STOP1-.05) 211,211,417
C     THE EFFECTIVE FLOW QUANTITIES AND PARAMETERS ARE CALCULATED FOR
C     A GIVEN FRACTION 'F' OF THE EFFECTIVE QF ACTUALLY BEING GAS.
211   QG=QGS-F*QFS/(1.-F)
      QF=QFS/(1.-F)
      ROF=ROFS*(1.-F)+ROG*F
      NU=NUS*ROFS/ROF
      BETAP=BETA/3.1415927*180.
      WRITE(3,400) BETAP,QFS,QGS,AVP
400   FORMAT('1',13X,'BETA=',F5.2,' DEGREES   QF=',F9.6,' FT**3/SEC   QG
     1=',F9.6,' FT**3/SEC   AVP=',F7.2,' LBF/IN**2',///)
      WRITE(3,402) DELR,RST,ROFS,ROG,NUS
402   FORMAT(8X,'DELR=',F5.3,' FT   RSTART=',F7.5,' FT   ROF=',F7.4,' LB
     1M/FT**3   ROG=',F7.4,' LBM/FT**3   NU=',E9.3,' FT**2/SEC',///)
      WRITE(3,415) QF,QG,ROF,NU
415   FORMAT(11X,'QFP=',F9.6,' FT**3/SEC   QGP=',F9.6,' FT**3/SEC   ROFP
     1=',F7.4,' LBM/FT**3   NUP=',E9.3,' FT**2/SEC',///)
      WRITE(3,408) K1,K2,K3,EPSI1,EPSI2,EPSI3,STOP
408   FORMAT(20X,'K1=',F4.1,'   K2=',F4.2,'   K3=',F4.2,'   EPSI1=',F5.3
     1,'   EPSI2=',F4.1,'   EPSI3=',F6.4,'   STOP=',F3.0,///)
      WRITE(3,416) F,FST,DELF,STOP1
416   FORMAT(36X,'F=',F5.3,'   FSTART=',F5.3,'   DELF=',F5.3,'   STOP1='
     1,F3.0,////)
      WRITE(3,403)
403   FORMAT(6X,'R',10X,'VB',9X,'V',8X,'ALPHA',8X,'LB',8X,'DPS',8X,'DPB'
     1,8X,'DPF',8X,'DPGR',7X,'DPM',9X,'DP',//)
      WRITE(3,404)
404   FORMAT(5X,'(FT)',5X,'(FT/SEC)',3X,'(FT/SEC)',16X,'(FT)',8X,'------
     1-------------- (LBF/FT**2/FT) --------------------',///)
      R=RST
      DO 401 I=1,20
      AI=I
      IF(AI-STOP-.05) 229,229,401
229   CONTINUE
```

```
      A=3.1415927*R*R
      LS=K1*R
      V=(QF+QG)/A
      VB=K2*V+K3*.35*SQRT(64.4*R*(ROF-ROG)/ROF)
C     THE FOLLOWING CALCULATES THE Z POSITION AT WHICH THE ACCELERATING
C     FORCE OF GRAVITY IS JUST BALANCED BY THE WALL SHEAR STRESS.
      Z=0.0
      DELZ=R/10.
201   Z=Z+DELZ
      IF(Z-2.*R)225,226,226
226   Z=Z-2.*DELZ
      DELZ=DELZ/10.
      GOTO 201
225   CONTINUE
      AG=FAG(Z)
      PF=FPF(Z)
      AF=A-AG
      YY1=ROF*SIN(BETA)
      Y1=-TAU(AG,PF)*PF/AF-YY1
      IF(ABS(Y1)-EPSI1*YY1) 205,205,207
207   IF(Y1) 201,205,204
204   Z=Z-2.*DELZ
      DELZ=DELZ/10.
      GOTO 201
205   ZS=Z
C     THE FOLLOWING IS THE CALCULATION OF THE GEOMETRICAL RELATIONSHIP
C     BETWEEN THE BUBBLE VOLUME AND THE BUBBLE LENGTH, USING A
C     BERNOULLI CONSTANT PRESSURE SURFACE FOR THE BUBBLE NOSE, A
C     HORIZONTAL SURFACE FOR THE BUBBLE TAIL AND A CONSTANT Z SURFACE
C     ( AT ZS ) IF NEEDED IN THE MIDDLE.
      XT1=0.0
      XN1=0.0
      SUMFB=0.0
      XP=0.0
      Z=0.0
      VOL=0.0
      L=LS
      DELZ=R/EPSI2
300   Z=Z+DELZ
      IF(Z-ZS)301,302,302
301   XT=Z*COS(BETA)/SIN(BETA)
      DELXT=XT-XT1
      XN=((VB*A/(A-FAG(Z)))**2-VB**2)/(64.4*SIN(BETA))-Z*COS(BETA)/SIN(B
     1ETA)
      IF(XN) 309,309,310
309   XN=0.
310   CONTINUE
      DELXN=XN-XN1
      L=L+DELXT+DELXN
      DVOL=FAG(Z-DELZ/2.)*(DELXT+DELXN)
      VOL=VOL+DVOL
C     THE GEOMETRICAL RELATIONSHIP AND A FLOW RELATIONSHIP BETWEEN
C     THE BUBBLE LENGTH AND THE BUBBLE VOLUME ARE SOLVED FOR A COMMON
C     SOLUTION.
      Y3=QG*A*L/(QF+QG+VB*A)-VOL
      IF(Y3)303,304,305
C     THE WALL FRICTION FORCES ARE SUMMED UNTIL THE ABOVE COMMON
C     SOLUTION IS FOUND.
305   AG=FAG(Z-DELZ/2.)
      PF=FPF(Z-DELZ/2.)
```

```
      SUMFB=SUMFB+TAU(AG,PF)*PF*(DELXT+DELXN)
      XN1=XN
      XT1=XT
      GOTO 300
303   IF(DELXT-EPSI3)306,306,307
306   IF(DELXN-EPSI3)304,304,307
307   L=L-DELXT-DELXN
      VOL=VOL-DVOL
      Z=Z-DELZ
      DELZ=DELZ/10.
      GOTO 300
304   AG=FAG(Z-DELZ/2.)
      PF=FPF(Z-DELZ/2.)
      SUMFB=SUMFB+TAU(AG,PF)*PF*(DELXT+DELXN)
      GOTO 308
C     THE LENGTH, VOLUME AND FRICTION FORCE ARE CALCULATED FOR THE
C     CONSTANT Z SURFACE WHEN IT IS NEEDED.
302   Z=ZS
      AG=FAG(Z)
      XP=Y3/(AG-QG*A/(QF+QG+VB*A))
      L=L+XP
      VOL=VOL+XP*AG
      PF=FPF(Z)
      SUMFB=SUMFB+TAU(AG,PF)*PF*XP
C     THE FRICTION FORCE ON THE SLUG OF FLUID BETWEEN BUBBLES IS
C     CALCULATED.
308   AG=FAG(0.)
      PF=FPF(0.)
      FS=TAU(AG,PF)*PF*LS
C     THE VOID FRACTION AND THE GRAVITY FORCE ALONG THE PIPE ARE
C     CALCULATED.
      ALPHA=QG/(QF+QG+VB*A)
      ROAV=ROF*(1.-ALPHA)+ROG*ALPHA
      FG=ROAV*A*L*SIN(BETA)
C     THE PRESSURE GRADIENTS ARE CALCULATED.
      DP=(SUMFB+FS+FG)/(A*L)
      DPF=(SUMFB+FS)/(A*L)
      DPGR=FG/(A*L)
      DPS=FS/(A*L)
      DPB=SUMFB/(A*L)
      SDP=DP
      SDPM=0.
      QUAL=QG*ROG/(QG*ROG+QF*ROF)
      SPV1=QUAL/ROG+(1.-QUAL)/ROF
      II=1
313   ROG2=ROG*(AVP*144.-DP)/(AVP*144.)
      SPV2=QUAL/ROG2+(1.-QUAL)/ROF
      G=(ROG*QG+ROF*QF)/A
      DPM=G*G*(SPV2-SPV1)/32.2
      DP=SDP+DPM
      IF(ABS((DPM-SDPM)/DPM)-.05) 311,311,312
312   SDPM=DPM
      II=II+1
      IF(II-6) 313,313,311
311   LB=L-LS
      RR=R+.0000001
      WRITE(3,405)RR,VB,V,ALPHA,LB,DPS,DPB,DPF,DPGR,DPM,DP
405   FORMAT(3X,F7.5,1X,10(1X,E10.3)//)
```

```
PAGE   6    BONDERSON

      R=R+DELR
401   CONTINUE
      F=F+DELF
417   CONTINUE
      GOTO 199
406   CALL EXIT
      END

FEATURES SUPPORTED
 IOCS

CORE REQUIREMENTS FOR SLUG
 COMMON      12  VARIABLES     160  PROGRAM    1650

 END OF COMPILATION

// XEQ
```

BETA=10.00 DEGREES   QF= 0.020000 FT**3/SEC   QG= 0.100000 FT**3/SEC   AVP= 14.70 LBF/IN**2

DELR=0.010 FT   RSTART=0.04000 FT   ROF=62.2400 LBM/FT**3   ROG= 0.0750 LBM/FT**3   NU=0.100E-04 FT**2/SEC

QFP= 0.020000 FT**3/SEC   QGP= 0.100000 FT**3/SEC   ROFP=62.2400 LBM/FT**3   NUP=0.999E-05 FT**2/SEC

K1=20.0   K2=0.20   K3=1.00   EPSI1=0.020   EPSI2=30.0   EPSI3=0.0005   STOP=11.

F=0.000   FSTART=0.000   DELF=0.000   STOP1= 1.

R	VB	V	ALPHA	LB	DPS	DPB	DPF	DPGR	DPM	DP
(FT)	(FT/SEC)	(FT/SEC)		(FT)	-------------------- (LBF/FT**2/FT) --------------------					
0.04000	0.533E 01	0.238E 02	0.681E 00	0.724E 02	0.121E 01	0.131E 02	0.144E 02	0.345E 01	0.141E 01	0.192E 02
0.05000	0.368E 01	0.152E 02	0.671E 00	0.350E 02	0.105E 01	0.395E 01	0.501E 01	0.355E 01	0.264E 00	0.883E 01
0.06000	0.280E 01	0.106E 02	0.658E 00	0.213E 02	0.847E 00	0.132E 01	0.217E 01	0.369E 01	0.858E-01	0.595E 01
0.07000	0.230E 01	0.779E 01	0.643E 00	0.151E 02	0.641E 00	0.441E 00	0.108E 01	0.386E 01	0.387E-01	0.498E 01
0.08000	0.198E 01	0.596E 01	0.625E 00	0.119E 02	0.472E 00	0.985E-01	0.570E 00	0.405E 01	0.211E-01	0.465E 01
0.09000	0.178E 01	0.471E 01	0.604E 00	0.100E 02	0.344E 00	-0.483E-01	0.295E 00	0.428E 01	0.130E-01	0.459E 01
0.10000	0.165E 01	0.381E 01	0.581E 00	0.885E 01	0.252E 00	-0.114E 00	0.137E 00	0.452E 01	0.872E-02	0.467E 01
0.11000	0.156E 01	0.315E 01	0.557E 00	0.800E 01	0.186E 00	-0.142E 00	0.445E-01	0.479E 01	0.617E-02	0.484E 01
0.12000	0.150E 01	0.265E 01	0.531E 00	0.735E 01	0.140E 00	-0.150E 00	-0.101E-01	0.506E 01	0.455E-02	0.506E 01
0.13000	0.146E 01	0.226E 01	0.505E 00	0.682E 01	0.107E 00	-0.148E 00	-0.416E-01	0.534E 01	0.347E-02	0.531E 01
0.14000	0.144E 01	0.194E 01	0.479E 00	0.639E 01	0.829E-01	-0.141E 00	-0.588E-01	0.563E 01	0.271E-02	0.557E 01

APPENDIX C

A pipeline designer would not be interested in minimizing the pressure gradient, but instead would think in terms of minimizing the total cost of construction and operation of a pipeline over a period of time.

For a typical set of pipeline flow rates a determination will be made of how close the total cost minimum is to the pressure gradient minimum. It will be assumed that for reasonably small changes in pipe size the only change in the cost of constructing the pipeline is due to the cost of the materials. All material costs and pumping station construction costs will be spread over a 20 year lifetime.

The system variables used were:

Oil and Natural Gas

$\beta = 10^{o}$

$Q_f = .426\ Ft^3/SEC.$

$Q_g = 1.87\ FT^3/\ SEC.$

$\rho_f = 48.7\ LB_m/FT^3.$

$\rho_g = 3.32\ LB_m/FT^3.$

$\eta_f = 7.94 \times 10^{-6}\ FT^2/SEC.$

The Model Parameters were:

K_1	=	20.
K_2	=	.20
K_3	=	1.74
F	=	0.

The model predicted the following pressure gradients close to the minimum:

ΔP, in LB_f/FT^3	R in FT.
4.68	.20
4.28	.25
4.39	.30
4.67	.35

The following expression for the cost will be minimized:

$$\frac{\text{COST}}{\text{FT YEAR}} = \frac{\text{PIPE COST + STATION COST + PUMPING COST}}{\text{FT} \quad \text{YEAR}}$$

$$= \frac{\text{PIPE COST}}{\text{FT YEAR}} + \Delta P \times \frac{\text{HP}}{\text{FT } \Delta P} \times \left(\frac{\text{STATION COST}}{\text{HP YEAR}} + \frac{\text{PUMPING COST}}{\text{HP YEAR}} \right) \quad \text{(C 1)}$$

The pipeline material cost data from Reference 13 was plotted on logarithmic graph paper. The data was very well approximated by the equation:

$$\frac{\text{PIPE COST}}{\text{FT}} = \$11.26\ R^{9/7} \quad ,$$

or for a 20 year lifetime:

$$\frac{\text{PIPE COST}}{\text{FT YEAR}} = \$\ .563\ R^{9/7} \quad .$$

From the same reference a reasonable approximation for the cost of constructing a pumping station was found to be:

$$\frac{\text{STATION COST}}{\text{HP YEAR}} = \$17.50 \quad ,$$

for a 20 year lifetime.

For a $Q = Q_f + Q_g = 2.30\ FT^3/\ SEC$, the horsepower needed for a pump efficiency of 80% is:

$$HP = \frac{(FT)\ (\Delta P)\ (Q)}{(550)\ (.80)} \quad ,$$

or

$$\frac{HP}{FT\ \ \Delta P} = .00522$$

It should be noted in all equations that ΔP is a pressure gradient while (FT) (ΔP) is a pressure drop.

Assuming a power cost of \$.01/KWHR and a motor efficiency of 80% one finds:

$$\frac{\text{PUMPING COST}}{\text{HP YEAR}} = \frac{\$.01}{\text{KWHR}} \times \frac{\text{KWHR}}{1.341 \text{ HP-HR}} \times \frac{1}{.80} \times \frac{8760 \text{ HR}}{\text{YEAR}}$$

$$= \$81.70$$

Eq. (C 1) then becomes:

$$\frac{\text{COST}}{\text{FT YEAR}} = \$.563^{9/7} + \$.518\ \Delta P\ .$$

To minimize this cost expression with respect to pipe size requires:

$$\frac{d}{dR}\left(\frac{\text{COST}}{\text{FT YEAR}}\right) = 0\ .$$

Thus one obtains:

$$\frac{d}{dR}\ (\Delta P) = -1.4\ R^{2/7}\ . \qquad \text{(C 2)}$$

The pressure gradient versus pipe size results listed previously may be approximated by a parabola in the vicinity of the minimum pressure gradient. The expression:

$$\Delta P - 4.26 = 102(R - .264)^2$$

perfectly satisfies the three points closest to the minimum pressure gradient. Thus, using this parabolic curve fit the minimum pressure gradient is estimated to be $\Delta P = 4.26\ lb_f/ft^3$ at $R = .264$ ft.

From this expression one can obtain:

$$\frac{d}{dR}(\Delta P) = 204(R - .264) \quad .$$

Eq. (C 2) then becomes:

$$204(R - .264) = -1.4 \quad R^{2/7} \quad .$$

This may be solved graphically or by trial and error to obtain:

$$R = .259 \text{ ft.}$$

This value of the optimum pipe size is only 1.9% smaller than the optimum pipe size as found by minimizing only the total pressure gradient.

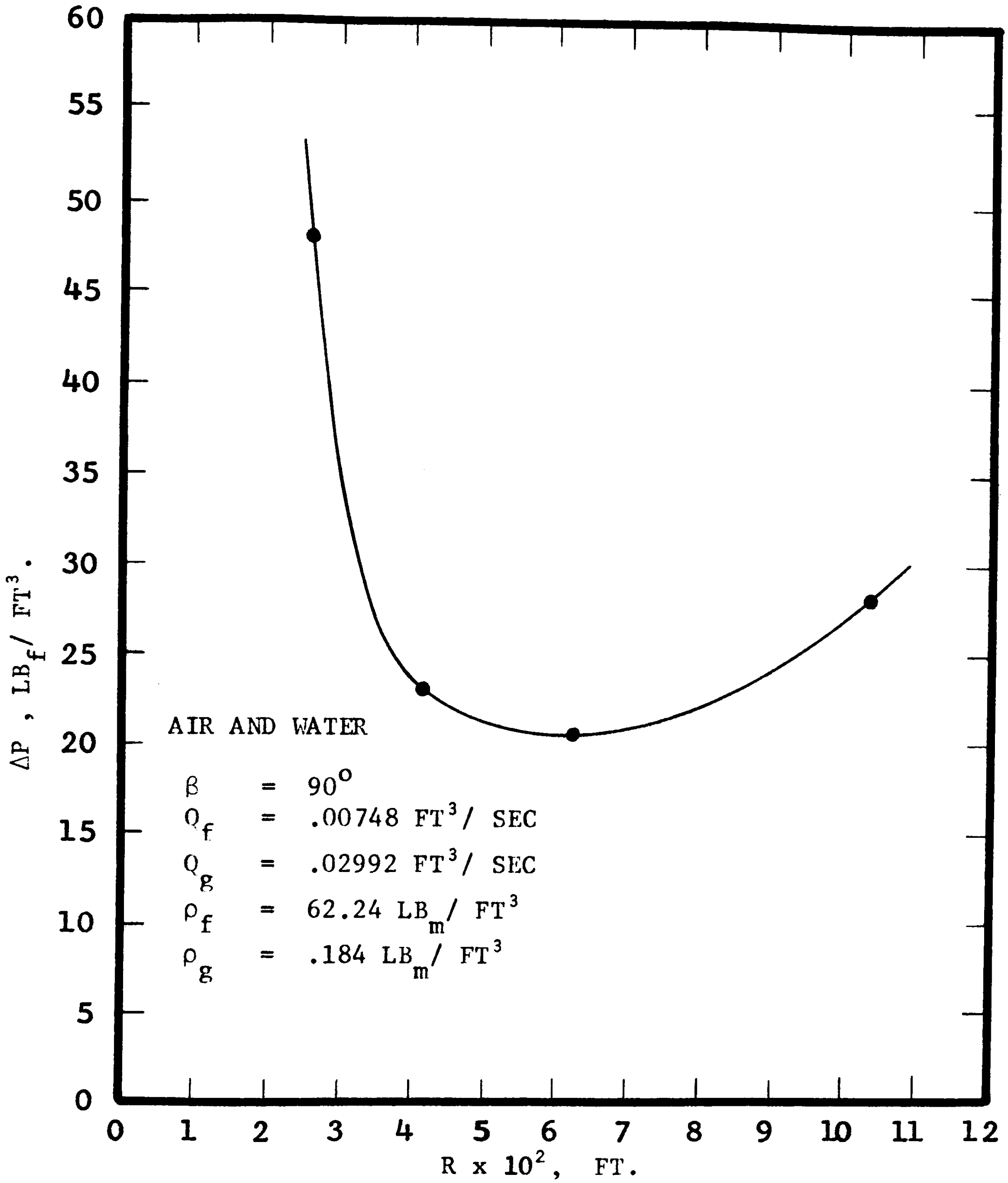

Figure 1. EXISTENCE OF MINIMUM PRESSURE GRADIENT FOR FIXED VOLUME FLOW RATES.

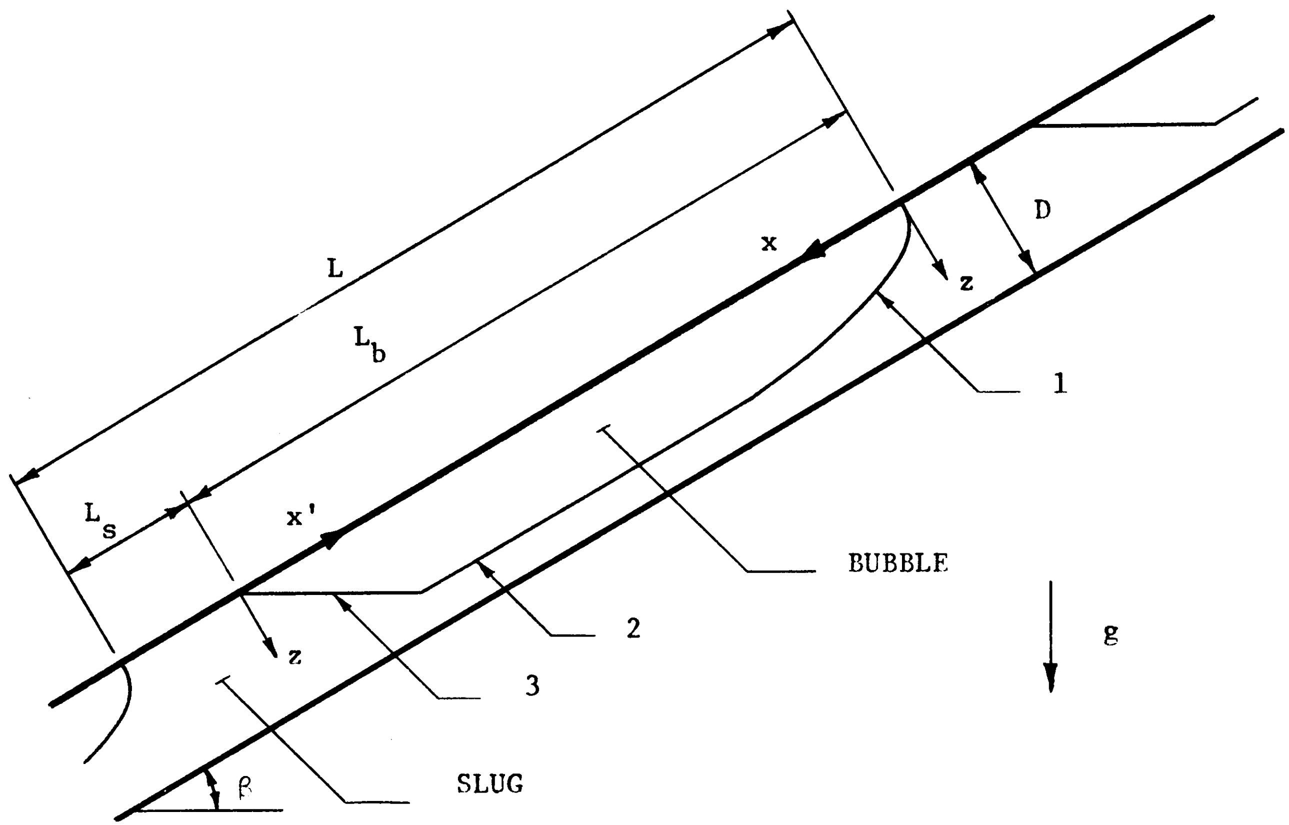

Figure 2.   MODEL VISUALIZATION

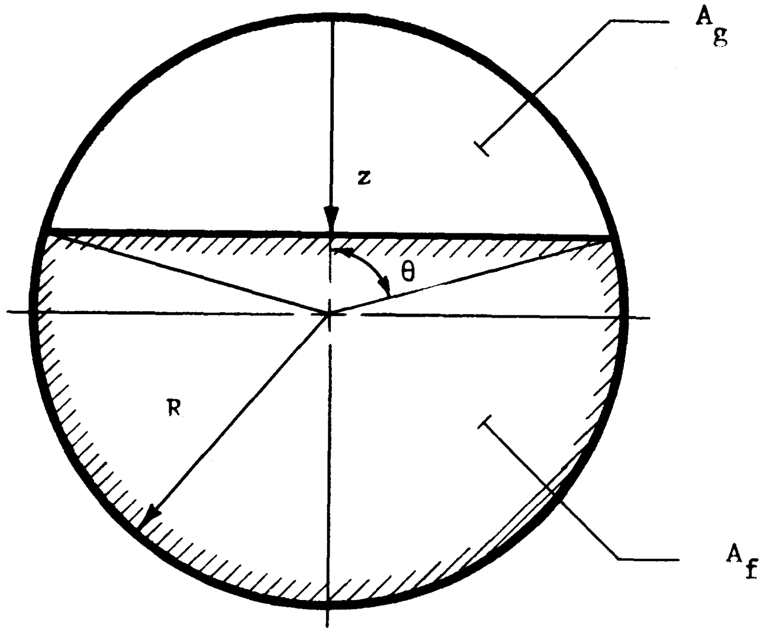

Figure 3. CROSS SECTION GEOMETRY

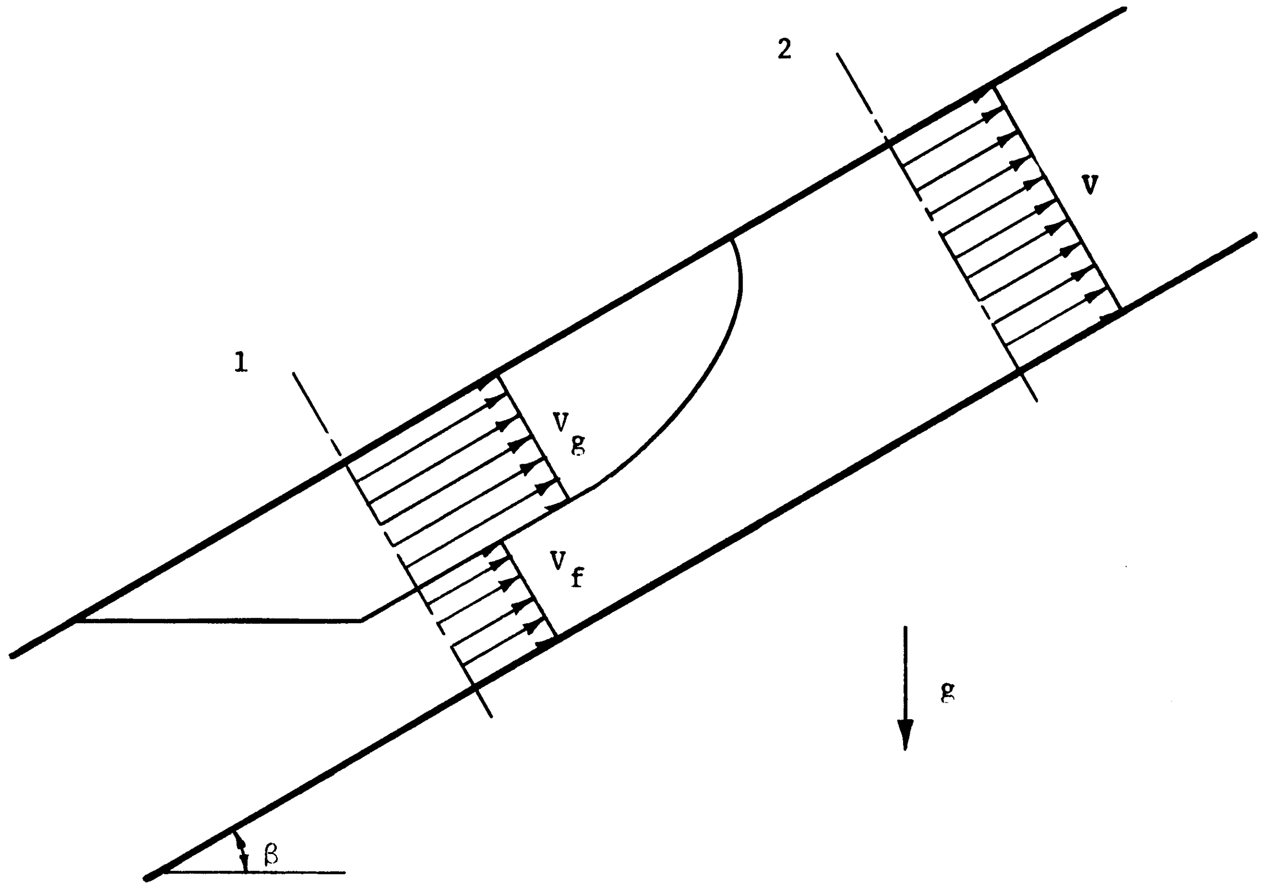

Figure 4. PHASE VELOCITIES

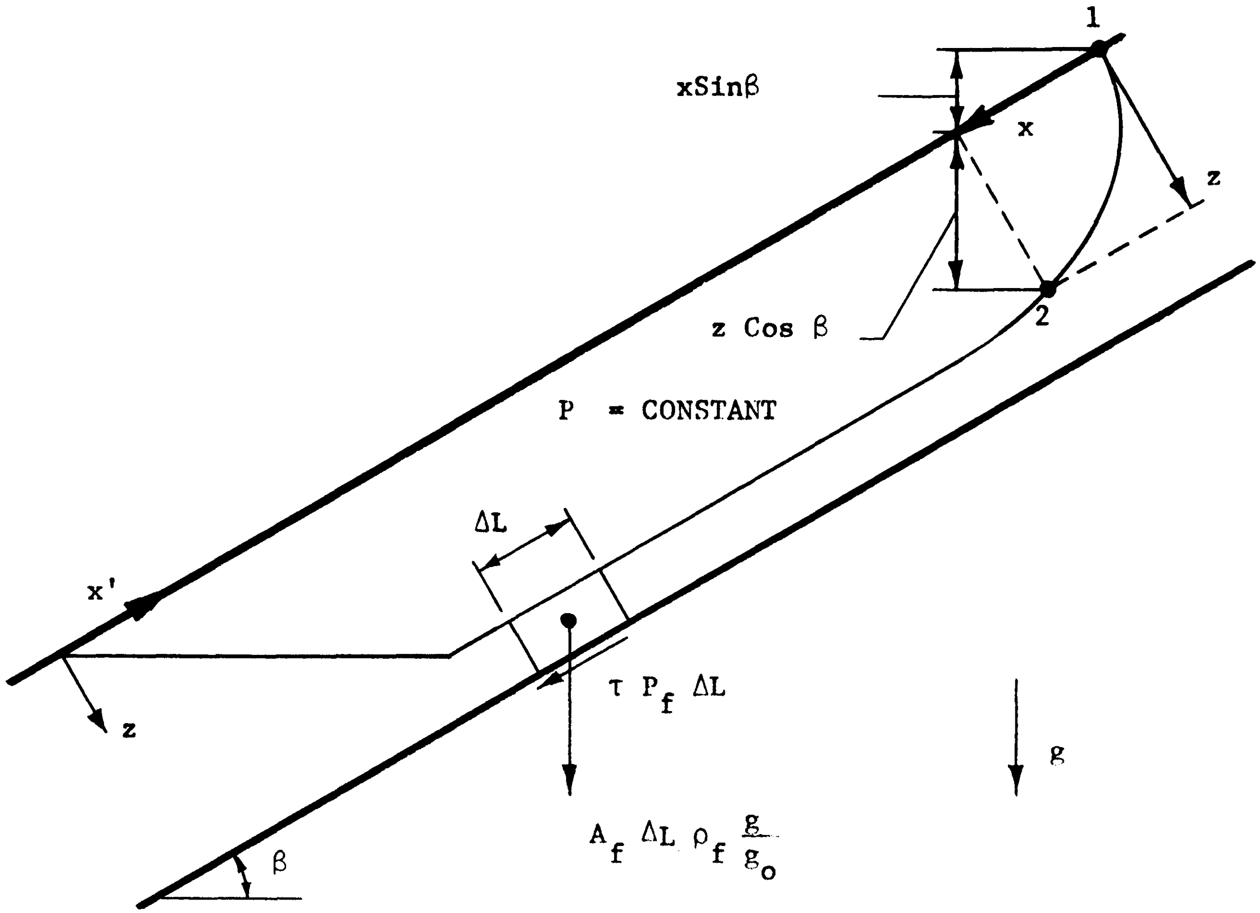

Figure 5. FORCE AND DISTANCE QUANTITIES

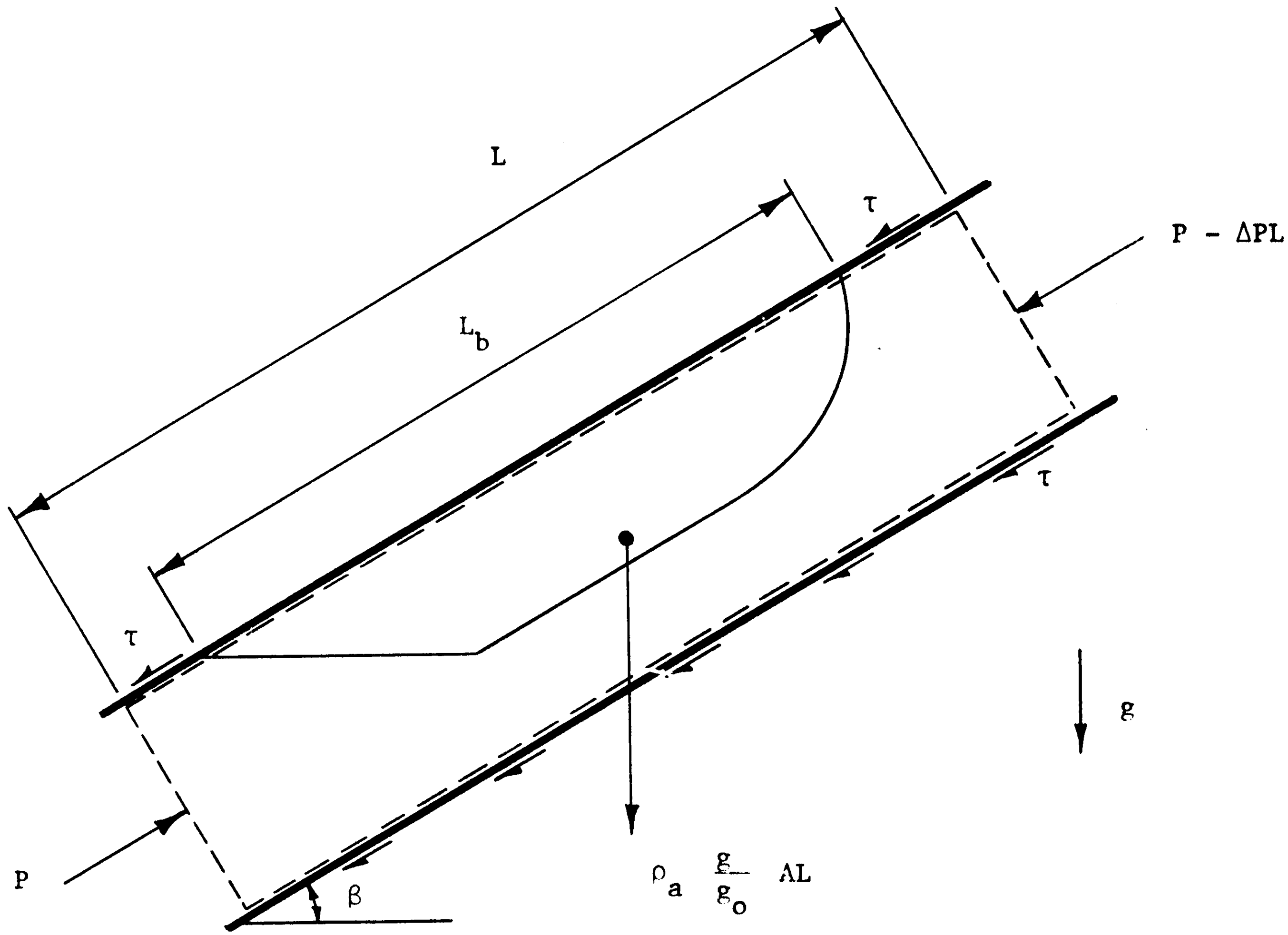

Figure 6. CONTROL VOLUME FOR PRESSURE GRADIENT ANALYSIS

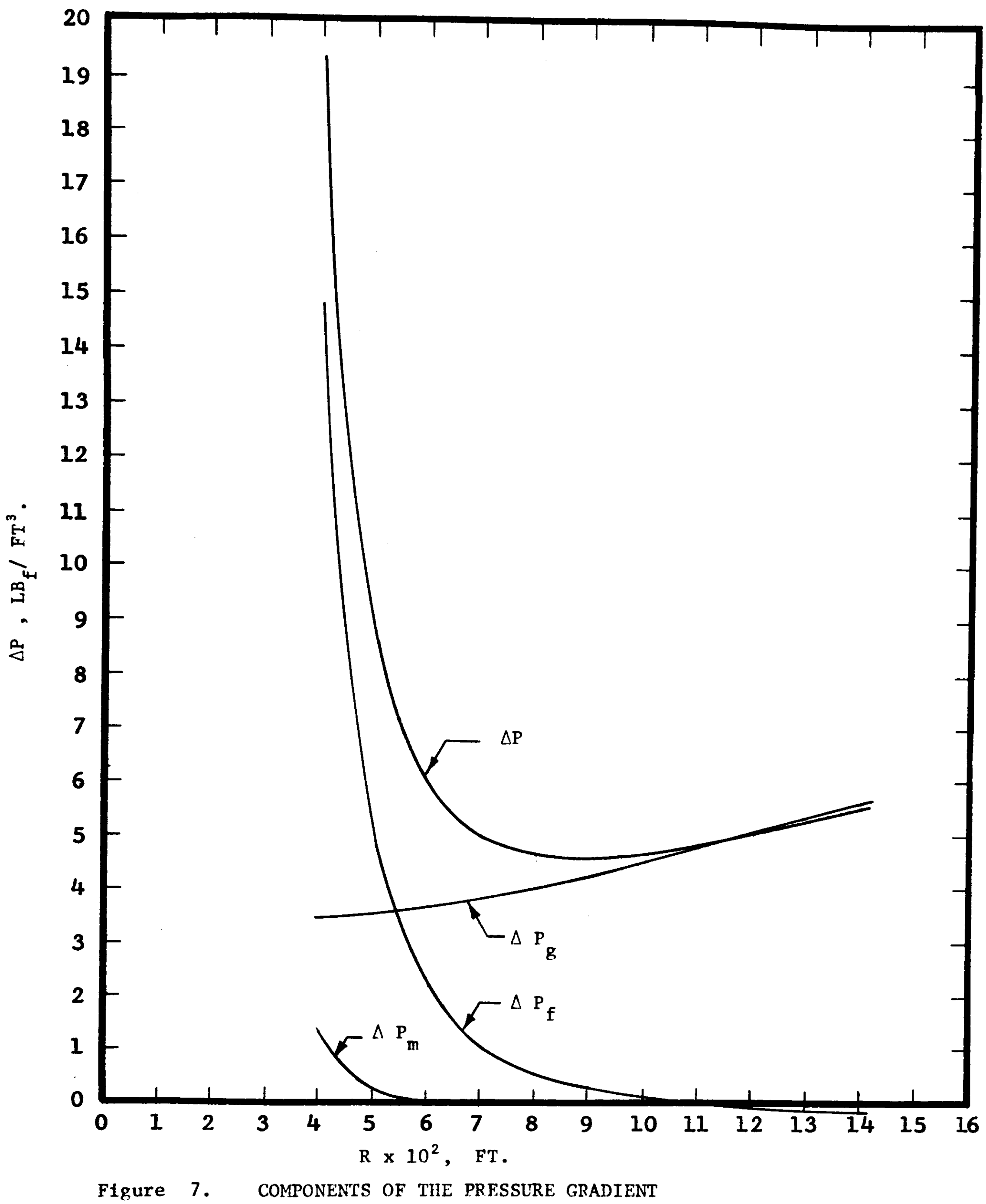

Figure 7. COMPONENTS OF THE PRESSURE GRADIENT

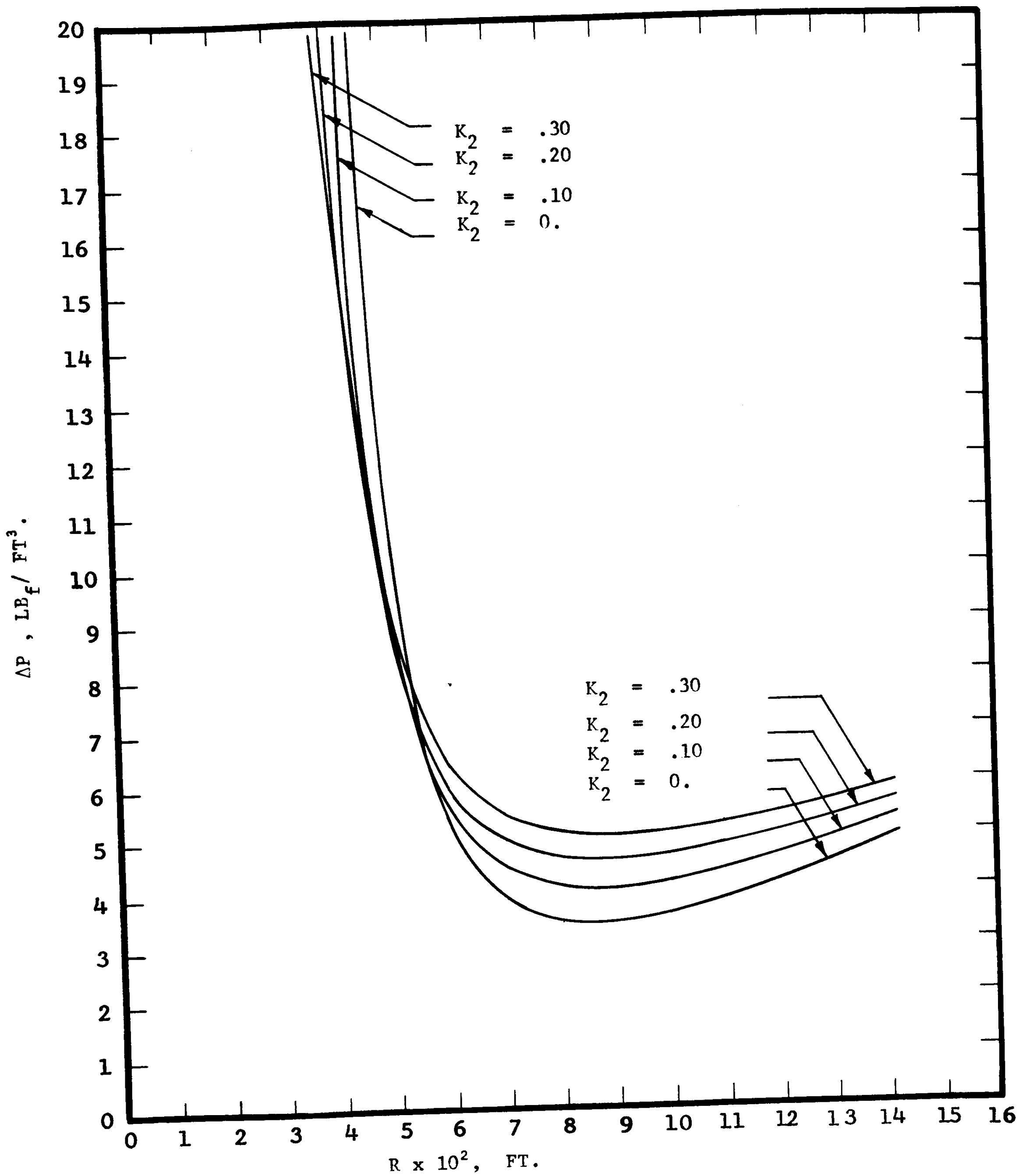

Figure 9. PRESSURE GRADIENT DEPENDENCE ON MODEL PARAMETER K_2.

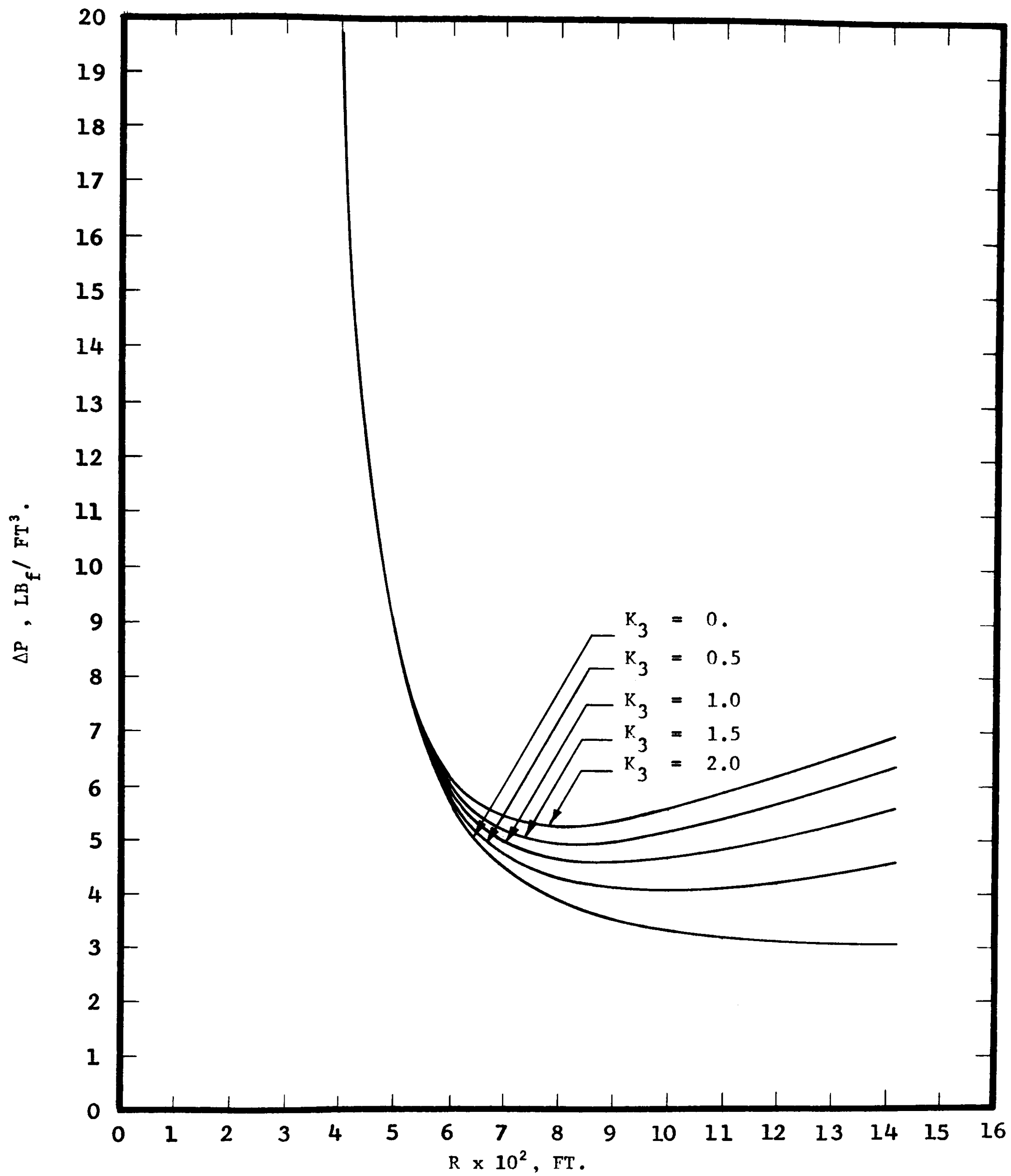

Figure 10. PRESSURE GRADIENT DEPENDENCE ON MODEL PARAMETER K_3.

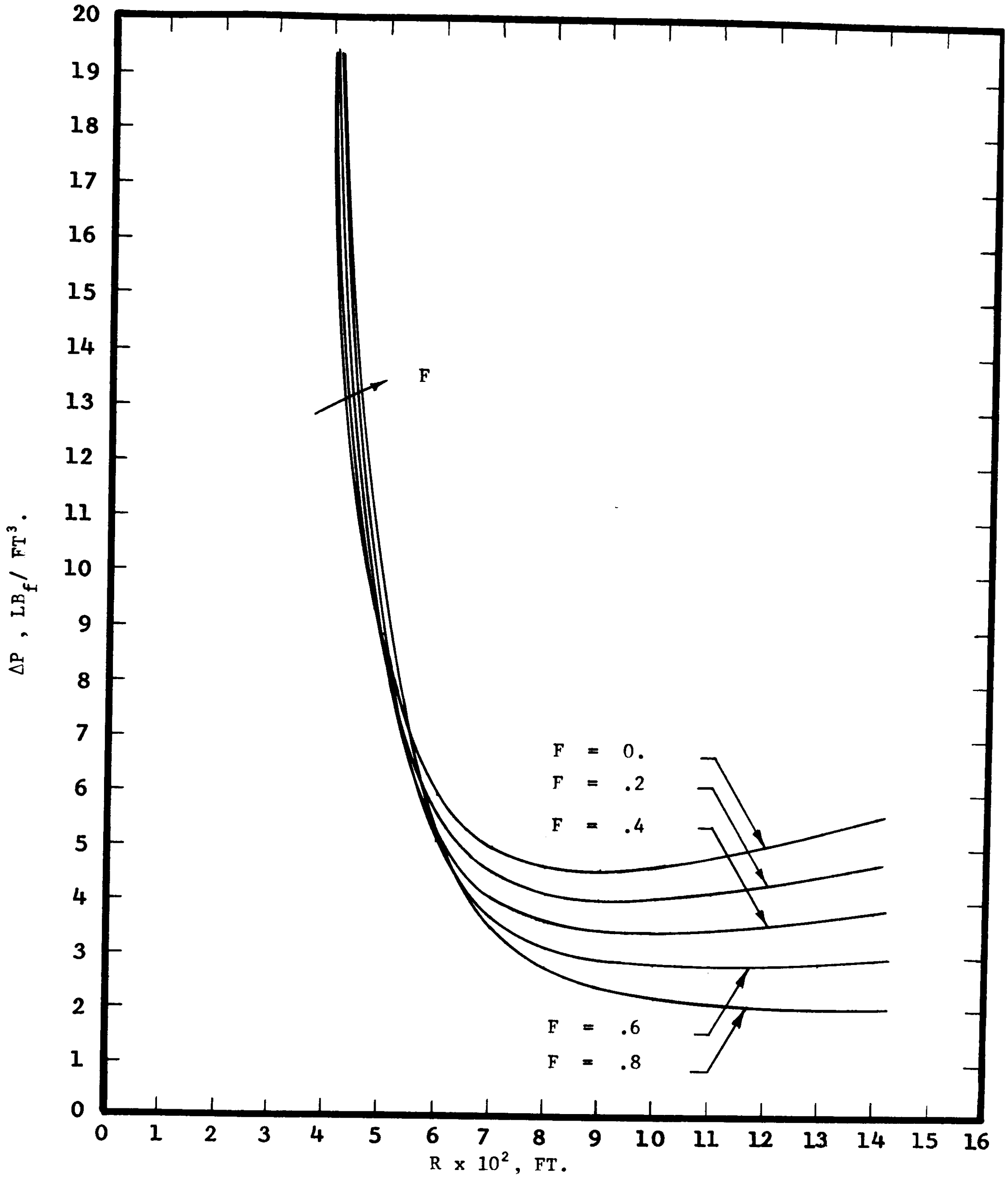

Figure 11. PRESSURE GRADIENT DEPENDENCE ON MODEL PARAMETER F.

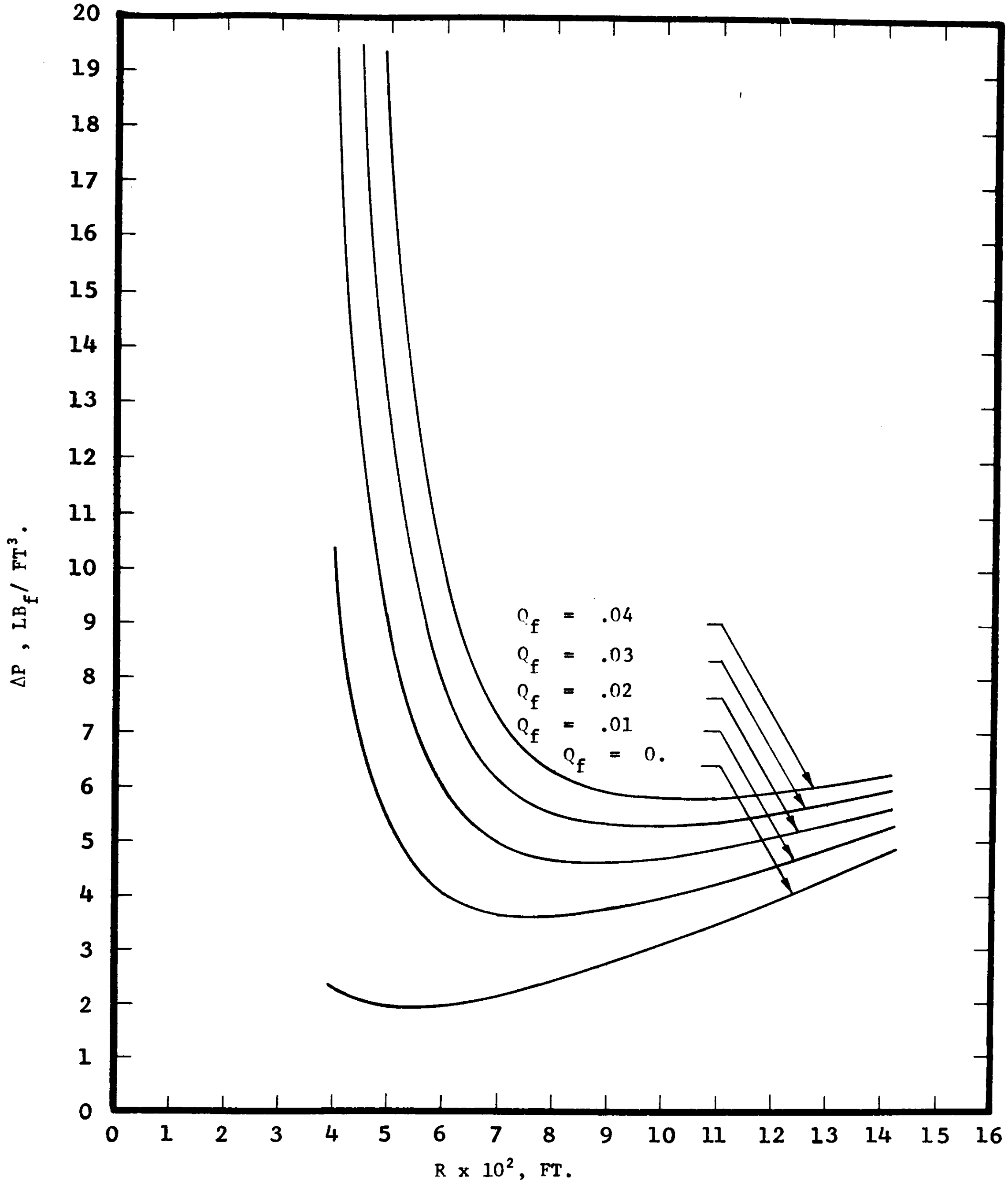

Figure 12. PRESSURE GRADIENT DEPENDENCE ON LIQUID VOLUME FLOW RATE.

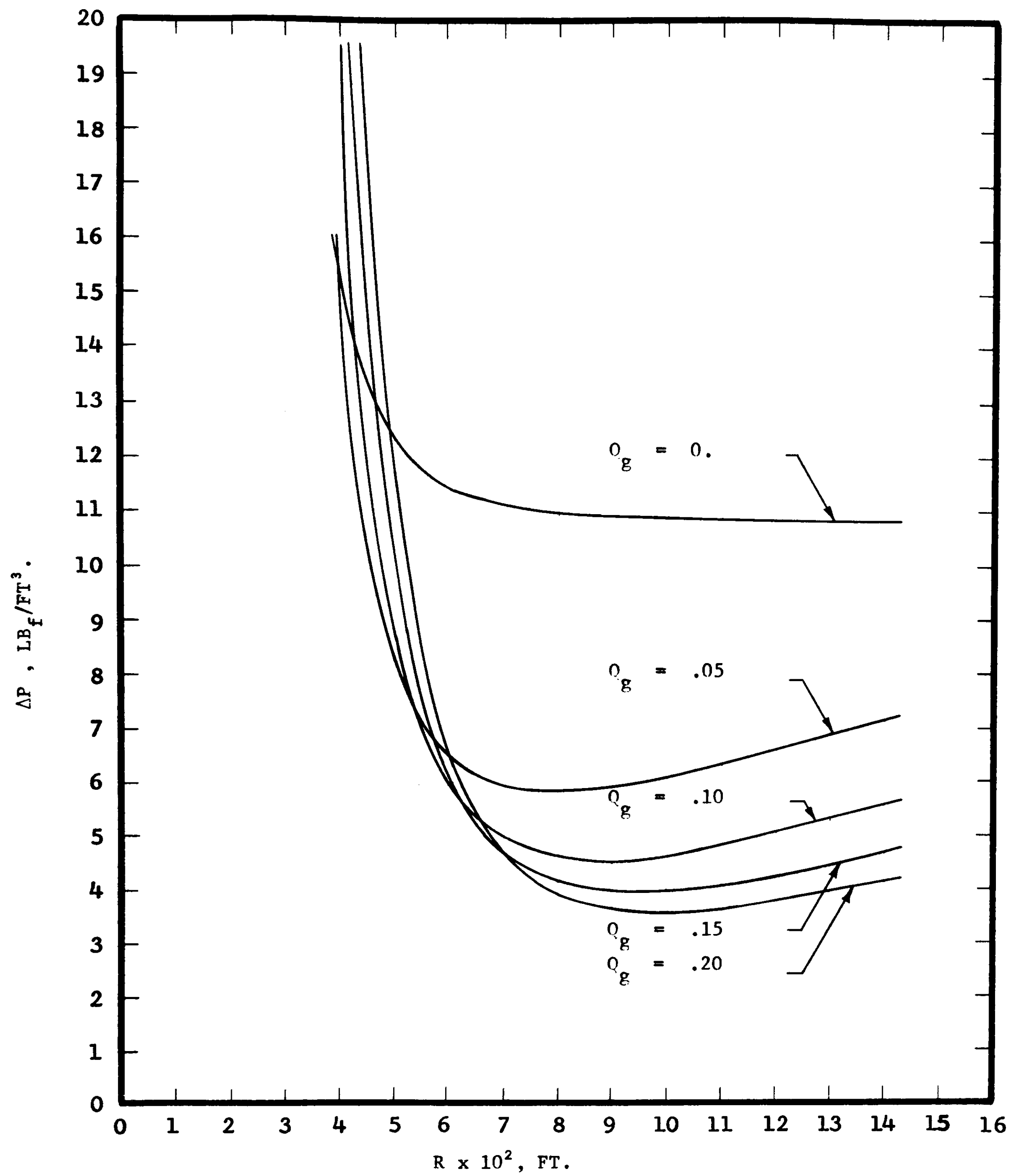

Figure 13. PRESSURE GRADIENT DEPENDENCE ON GAS VOLUME FLOW RATE.

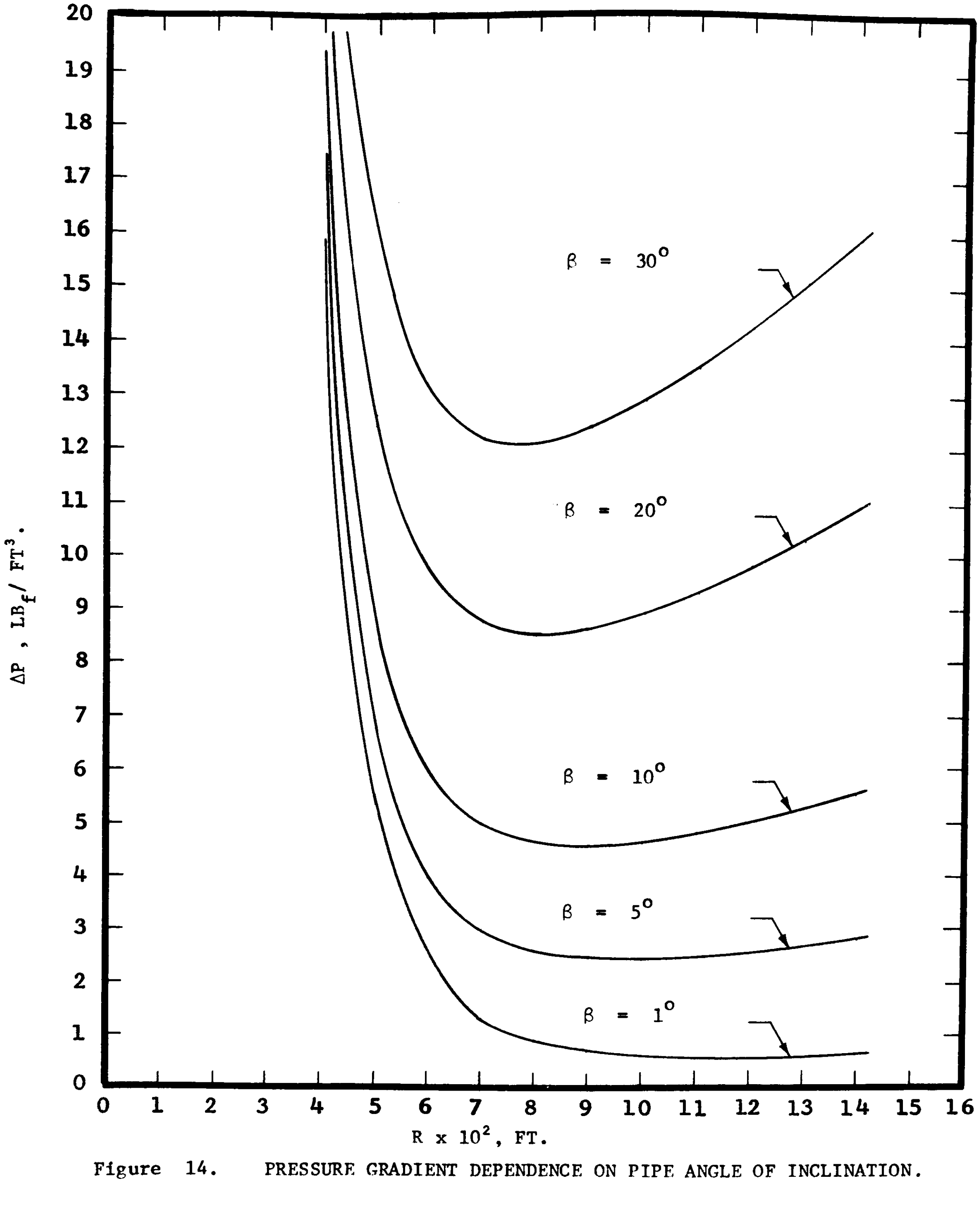

Figure 14. PRESSURE GRADIENT DEPENDENCE ON PIPE ANGLE OF INCLINATION.

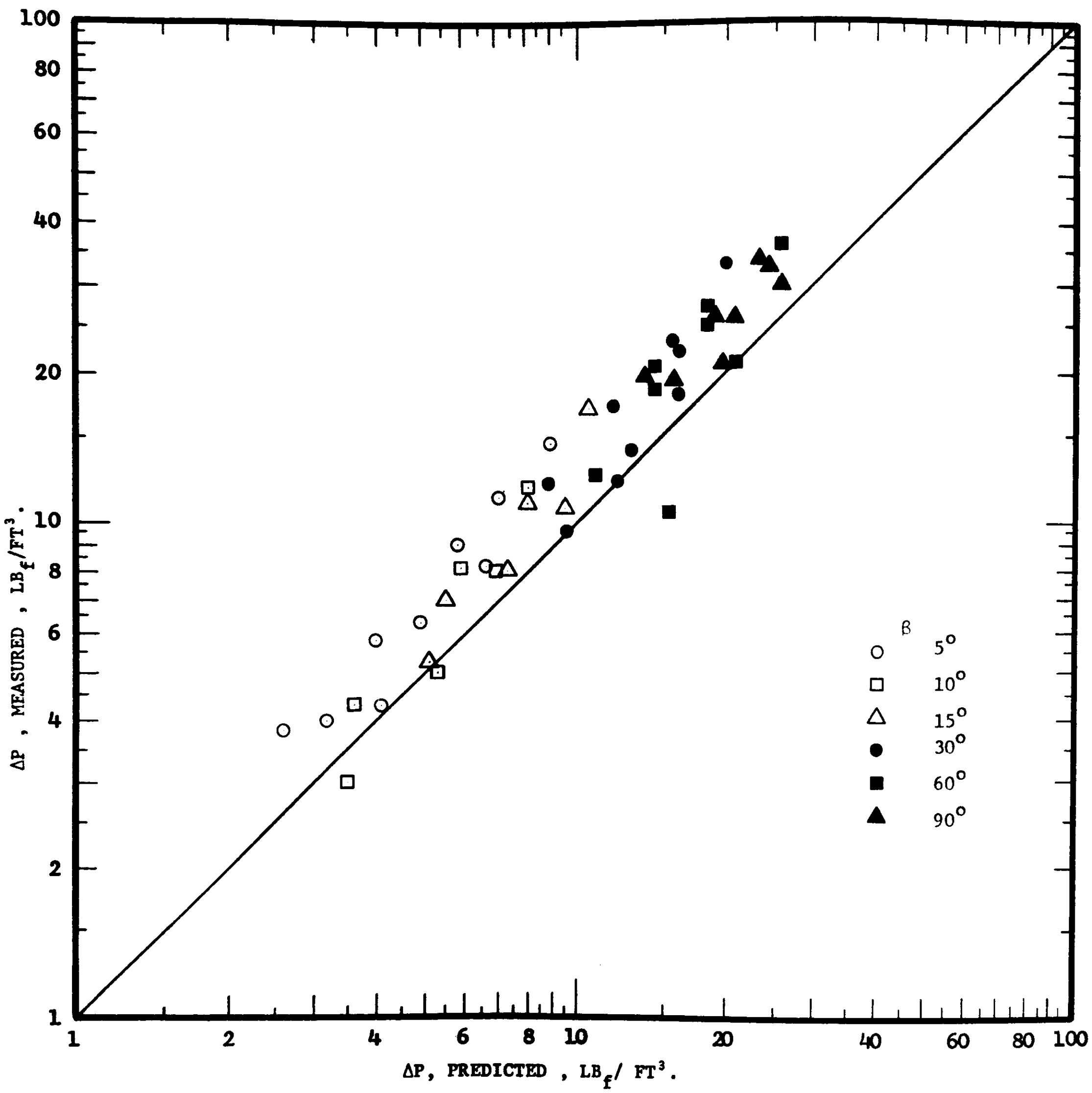

Figure 15. MEASURED PRESSURE GRADIENT VERSUS PREDICTED PRESSURE GRADIENT